

Power-suppressed contributions to deep-inelastic processes

J. F. Gunion

Department of Physics, University of California, Davis, California 95616

P. Nason and R. Blankenbecler

Stanford Linear Accelerator Center, Stanford University, Stanford, California 94305

(Received 11 July 1983; revised manuscript received 12 January 1984)

We present results of a direct calculation of leading power-law corrections to the proton and pion structure functions at large x to order $1/Q^4$ for νW_2^{proton} and $1/Q^2$ for W_L^{proton} and to order $1/Q^2$ for νW_2^{pion} and W_L^{pion} . For νW_2 we find large $\sim(1-x)^4$ corrections to the leading $\sim(1-x)^3$ behavior as $x \rightarrow 1$ and substantial $(1-x)^2/Q^2$ corrections, a phenomenologically desirable form. We find a very large value for the coefficient of $1/Q^2$ in $(\sigma_L/\sigma_T)^{\text{proton}}$. The $1/Q^2$ correction to νW_2^{pion} is of the form proposed by Berger and Brodsky but much smaller than their estimate after complete normalization constraints are imposed. In addition, this correction is not purely longitudinal until $(1-x)$ is very near zero.

INTRODUCTION

While QCD is widely accepted as the theory of the strong interactions, detailed comparison with experiment is far from perfect. Even the deep-inelastic structure function, which in principle provides one of the cleanest experimental tests, may have important power-law corrections at various orders in $1/Q^2$. Indeed, it now seems clear that the leading asymptotic terms predicted by QCD explain neither the low-to-moderate- Q^2 structure-function data nor the ratio $R = \sigma_L/\sigma_T$.^{1,2} In a previous Letter³ we presented partial results of a direct calculation of the leading power-law corrections to νW_2^{proton} and νW_L^{proton} at large x near 1 and large Q^2 . In the present paper we extend these calculations considerably. We calculate not only the leading $\sim(1-x)/Q^2$ correction to the $\sim(1-x)^3$ behavior of W_2^{proton} but also the $\sim 1/(1-x)Q^4$, the $\sim(1-x)^2/Q^2$ and scaling $(1-x)^4$ corrections. We find that (1) the $(1-x)/Q^2$ correction is small with negative coefficient, as previously reported; (2) the $1/(1-x)Q^4$ correction is small and positive; (3) both the $(1-x)/Q^2$ and $1/(1-x)Q^4$ corrections would vanish for a constant strong coupling constant—i.e., in a sense they derive from higher-order corrections; (4) the $(1-x)^2/Q^2$ correction is positive and of substantial magnitude; and (5) the $(1-x)^4$ correction is negative/positive for a proton/neutron target with large coefficient. Our asymptotic result for $\nu W_L^{\text{proton}}/\nu W_2^{\text{proton}}$ is, as previously reported, very large and x independent as $x \rightarrow 1$. (We note that the earlier calculations did not include helicity-flip contributions whereas those discussed here include all contributions in a given order.) This result for $\nu W_L^{\text{proton}}/\nu W_2^{\text{proton}}$ suggests that very large Q^2 is required before a meaningful asymptotic series for σ_L/σ_T can be developed. The size of all terms is fixed, in our approach, by the approximately known normalization of the leading $(1-x)^3$ term of νW_2^{proton} .

In the present paper we have also “repeated” the calculations of Berger and Brodsky¹⁴ for the $\sim(1-x)^2$ and

$\sim(1-x)^0/Q^2$ terms in νW_2^{pion} and the $(1-x)^0$ term in νW_L^{pion} . We have, however, included helicity-flip and other quark-mass effects. In addition, all normalizations are fixed by that of the $(1-x)^0/Q^2$ correction to νW_2^{pion} , which is much smaller than suggested in Ref. 4, and it is not purely longitudinal until x is extremely near 1.

We would like to emphasize that our purpose here is to perform a calculation within the context of the standard QCD picture of hadrons and not to give a detailed fit to data. At large x QCD predicts that the valence Fock states must dominate the hadron structure function. Our results for the valence Fock state will thus be valid for x sufficiently near 1. At moderate x it is likely that higher Fock states will be important. It is quite possible that the very large higher-twist effects that we obtain for the valence states are also present for those higher Fock states.

Our analysis will be based on the extension of the Brodsky-Lepage formalism⁵ first employed by Berger and Brodsky⁴ in their calculation of higher-twist contributions for pion beams. We begin in Sec. I by giving kinematic preliminaries. In Sec. II, we repeat the pion calculation using our techniques and discuss possible subtleties and difficulties in the original results. In Sec. III, we turn to the proton target.

I. KINEMATICS

We begin by giving a few kinematic preliminaries. The structure functions for deep-inelastic scattering are defined through

$$W_{\mu\nu}(p, q) = - \left[g_{\mu\nu} - \frac{q_\mu q_\nu}{q^2} \right] W_1 + \left[p_\mu - q_\mu \frac{p \cdot q}{q^2} \right] \left[p_\nu - q_\nu \frac{p \cdot q}{q^2} \right] W_2. \quad (1.1)$$

We use light-cone notation: for general vectors v and u we define

$$\begin{aligned}
v^+ &= v^0 + v^3, \quad v^- = v^0 - v^3, \\
\hat{v} &= v^1 + iv^2, \quad \check{v} = v^1 - iv^2, \\
\vec{v}_T &= (v_1, v_2), \\
v^2 &= v^+ v^- - \hat{v}\check{v} = v^+ v^- - v_T^2, \\
u \cdot v &= \frac{1}{2}(u^+ v^- + u^- v^+ - \hat{u}\check{v} - \check{u}\hat{v}).
\end{aligned} \tag{1.2}$$

Note that use of \hat{v} and \check{v} for transverse momenta will simplify later Dirac algebra.

In a frame defined by

$$q = (q^+, q^-, \vec{q}_T) \text{ with } q^+ = 0, \quad q^- = 2\nu/p^+, \quad q_T^2 = Q^2, \tag{1.3}$$

$$p = (p^+, p^-, \vec{Q}_T) \text{ with } p^- = M_{\text{target}}^2/p^+, \quad \nu = p \cdot q,$$

we have

$$W_2 = W^{++}/p^{+2}, \quad W_L = Q^2 p^{+2} \frac{W^{--}}{4\nu^2} \tag{1.4}$$

and the standard ratio of σ_L/σ_T is given by

$$\begin{aligned}
R &= \sigma_L/\sigma_T = \frac{r}{1-r}, \\
r &= \frac{4x_{\text{Bj}}^2}{Q^2} \left[\frac{\nu W_L}{\nu W_2} \right], \\
x_{\text{Bj}} &= \frac{Q^2}{2\nu}.
\end{aligned} \tag{1.5}$$

We will calculate W^{++} and W^{--} by computing the amplitudes, A^+ or A^- for absorption of a $+$ or $-$ component photon by the target, squaring the amplitude, and then integrating over final-state phase space. In computing A^+ or A^- , we begin by imagining a superposition of multiparticle Fock states⁵ for the incoming target. In the frame of Eq. (1.3), we define the amplitude for finding n (on-mass-shell) quarks and gluons with spin projection S_z along the z direction and momenta p_i as (see Fig. 1)

$$\psi_{S_z}^{(n)}(\alpha_i, \vec{p}_{Ti}, s_i), \quad \alpha_i = \frac{p_i^+}{p^+}, \tag{1.6}$$

where, by momentum conservation,

$$\sum_{i=1}^n \alpha_i = 1, \quad \sum_{i=1}^n \vec{p}_{Ti} = 0. \tag{1.7}$$

The s_i specify the spin projections of the constituents. For $x_{\text{Bj}} \rightarrow 1$ we will be concerned only with valence Fock states containing quarks or antiquarks. For each fermion or antifermion constituent $\psi_{S_z}^{(n)}$ multiplies the spin factor

$$\frac{u(\vec{p}_i)}{(p_i^+)^{1/2}} (p^+)^{1/2} \text{ or } \frac{\bar{v}(\vec{p}_i)}{(p_i^+)^{1/2}} (p^+)^{1/2}.$$

$$W^{+, -} = \left[\frac{1}{2} \right] \left[\frac{1}{2\pi} \right] \sum_{s_i'} \int \prod_{i=1}^n \frac{dx_i d^2 k_{Ti}}{2(2\pi)^3} 16\pi^3 \delta^2 \left[\sum_i \vec{k}_{Ti} \right] \delta \left[1 - \sum_i x_i \right] \frac{2\pi}{p^+} \delta \left[(p+q)^- - \sum_i k_i^- \right] |A^{+, -}|^2, \tag{1.10}$$

where $A^{+, -}$ depends on x_i , \vec{k}_{Ti} , and s_i' .

Finally, we sum over the possible quarks which can be struck by the deep-inelastic photon. We do not allow for

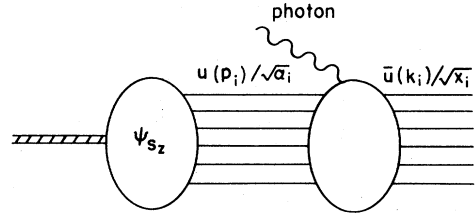


FIG. 1. The initial and final Fock states of a general bound state of fermions.

The wave function is normalized according to

$$\begin{aligned}
&\sum_{s_i} \int \prod_i^n \frac{d^2 p_{Ti} d\alpha_i}{2(2\pi)^3} \psi_{S_z}^{(n)}(\vec{p}_{Ti}, \alpha_i, s_i)^2 \\
&\quad \times 16\pi^3 \delta \left[1 - \sum \alpha_i \right] \delta^2 \left[\sum \vec{p}_{Ti} \right] = 1.
\end{aligned} \tag{1.8}$$

Our spinor normalization is such that

$$\sum_s u_s(p) \bar{u}_s(p) = \not{p} + m.$$

Similarly, the final state created by the absorption of a $+$ or $-$ component photon will be specified by momenta and spinors

$$\frac{\bar{u}(k_i)}{(k_i^+)^{1/2}} (p^+)^{1/2} \text{ or } \frac{\bar{v}(k_i)}{(k_i^+)^{1/2}} (p^+)^{1/2}$$

(see Fig. 1). In this normalization the phase space associated with an n -particle final state is $(x_i \equiv k_i^+/p^+)$

$$\begin{aligned}
d\Gamma^{(n)} &\equiv \sum_{s_i'} \prod_{i=1}^n \frac{dx_i d^2 k_{Ti}}{2(2\pi)^3} 16\pi^3 \delta^2 \left[\sum_i \vec{k}_{Ti} \right] \\
&\quad \times \delta \left[1 - \sum_i x_i \right] \frac{2\pi}{p^+} \delta \left[(p+q)^- - \sum_i k_i^- \right].
\end{aligned} \tag{1.9}$$

Our procedure will be to calculate W^{++} or W^{--} by first computing the amplitude A^+ or A^- for a given quark in the initial-state configuration specified by ψ_{S_z} to absorb a $+$ or $-$ component photon and yield a final state as specified above; this amplitude will include the integration over initial configurations \vec{p}_{Ti} and α_i and a coherent sum over the initial quark spin states for the given S_z . We then obtain, for a given struck quark,

interference terms in which the photon is absorbed on different quarks of the target. These terms are suppressed by a factor of

$$\frac{\alpha_s(Q^2)}{\alpha_s("k_T^{2"}/(1-x_{Bj}))}$$

relative to the diagonal terms we retain. This is because the virtual-photon momentum has to be routed through an explicit gluon exchange between the two interfering quarks (when visualizing the calculation as that of the imaginary part of the forward Compton amplitude). Our normalization is such that for a one-particle state $vW_2 = \delta(1-x_{Bj})$.

II. CALCULATIONAL FRAMEWORK AND APPLICATION TO PION STRUCTURE FUNCTION

We now consider deep-inelastic scattering on a pion target at large x_{Bj} . In the $x_{Bj} \rightarrow 1$ limit the bound-state quark struck by the virtual photon is required to carry most of the $+$ component of longitudinal momentum. The simplest diagrams allowing this configuration are illustrated in Fig. 2, where we consider the $q\bar{q}$ Fock component (in the light-cone decomposition of Ref. 5), higher Fock components being suppressed by powers of $(1-x_{Bj})^2$. We will calculate the amplitude for virtual-photon absorption in the $x_{Bj} \rightarrow 1$ limit and later square and provide phase-space factors to obtain the structure functions, as discussed in Sec. I.

In the frame of Eq. (1.3), the on-shell recoil momentum $p-k$ of Figs. 2(a)–2(b) is given by

$$\begin{aligned} (p-k)^+ &= (1-x)p^+, \\ (p-k)^- &= \frac{m^2 + k_T^2}{(1-x)p^+}, \\ (\vec{p}-\vec{k})_T &= -\vec{k}_T, \end{aligned} \quad (2.1)$$

where m is the spectator-quark mass and $x = x_{Bj}$ in leading order. From (2.1) we find that

$$k^2(x) \sim \frac{-(m^2 + k_T^2)}{(1-x)} \quad (2.2)$$

is forced far off-shell in the $x \rightarrow 1$ region. This purely kinematic result allows us to apply the Brodsky-Lepage formalism in the $x \rightarrow 1$ limit.^{5,4}

In the procedure of Ref. 5 one notes that the transverse momenta of the initial quarks do not enter into the large off-shell momentum (2.2). Thus one may evaluate the tree graphs of Figs. 2(a) and 2(b) with collinear on-shell initial quark and antiquark lines and incoming spinors,

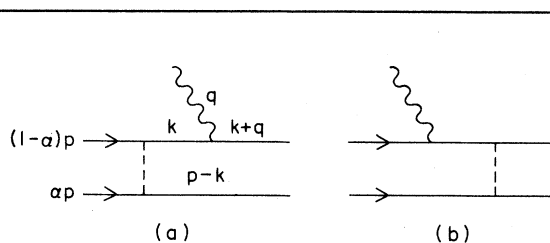


FIG. 2. Tree graphs for the two-quark pion valence state at large x_{Bj} .

$$\frac{u(\alpha p^+)}{\sqrt{\alpha}} \text{ and } \frac{\bar{v}[(1-\alpha)p^+]}{\sqrt{1-\alpha}}.$$

This tree-graph result is then convoluted with the evolved wave function $\phi(\alpha, "Q^{2"}$) defined by (for simplicity we do not write the standard wave-function renormalization factor)

$$\begin{aligned} \phi(\alpha, "Q^{2"}) &= \sum_{s_1 s_2} \int "Q^{2"} \frac{d^2 p_{T1} d^2 p_{T2}}{(16\pi^3)^2} 16\pi^3 \delta(\vec{p}_{T1} + \vec{p}_{T2}) \\ &\quad \times \psi_{S_2}(\vec{p}_1, \vec{p}_2, s_1, s_2) \delta(s_1 + s_2), \end{aligned} \quad (2.3)$$

where $p_1^+ \equiv \alpha p^+$, $p_2^+ \equiv (1-\alpha)p^+$, and we require a spin-0 $q\bar{q}$ Fock state for the pion. This "evolved" wave function is thus the integral over initial transverse momenta of the Fock-state wave function with upper limit " $Q^{2"}$ set by

$$"Q^{2"} \sim k^2(x). \quad (2.4)$$

This is the point beyond which the initial transverse momenta can no longer be neglected in calculating the tree graphs. It is the region below " $Q^{2"}$ which gives the leading-logarithmic contribution in the $x \rightarrow 1$ limit.⁵

In the limit of very large " $Q^{2"}$, $\phi(\alpha, "Q^{2"}$) takes a particularly simple form⁵ for a pion,

$$\phi(\alpha, "Q^{2"}) \underset{"Q^{2"} \rightarrow \infty}{\sim} \alpha(1-\alpha) \frac{3f\pi}{\sqrt{n_c}}, \quad (2.5)$$

where n_c = number of colors. At more moderate " $Q^{2"}$ the wave function will not have reached its fully evolved form. In fact, Berger and Brodsky⁴ use the weak-binding form

$$\phi(\alpha, "Q^{2"}) = \delta(\alpha - \frac{1}{2}) \frac{f\pi}{4} \frac{3}{\sqrt{n_c}}. \quad (2.6)$$

We have chosen the normalization of ϕ so that the normalization of the large- Q^2 pion form factor, proportional to $\int \phi(\alpha)/\alpha$,⁵ is the same for (2.5) and (2.6). More sophisticated forms for ϕ are considered in Ref. 6. We do not, in this paper, wish to explore all possibilities for the pion and so we will restrict our considerations to a ϕ of the form Eq. (2.6). We will employ $f_\pi = 130$ MeV.

The above wave function for momentum coordinates must be supplemented by the color wave function

$$\frac{\delta_{ab}}{\sqrt{n_c}} \quad (2.6')$$

(a, b = quark, anti-quark colors, respectively), and the pion spin wave function

$$\frac{1}{\sqrt{2}} (|+, -\rangle - |-, +\rangle), \quad (2.6'')$$

both normalized to unity in the square. The $+$ and $-$ refer to infinite- p^+ helicity states (see Ref. 5).

The calculation will employ an axial gauge for the gluon specified by

$$\eta \cdot A_{\text{gluon}} = 0, \quad \eta = (0, \eta^-, 0, 0). \quad (2.7)$$

In this gauge the rules for the numerator of the gluon propagator,

$$-g_{\mu\nu} + \frac{\eta_\mu k_\nu + \eta_\nu k_\mu}{\eta \cdot k} \equiv p_{\mu\nu}(k),$$

are specified in Table I.

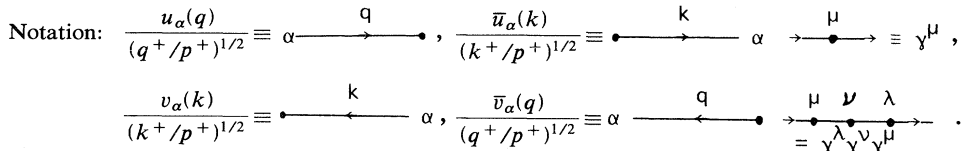
We will also employ the Dirac-algebra rules for matrix elements between on-shell spinors specified in Table II, adapted from Ref. 5 to our more convenient notation. We will employ "helicity" states where the helicity is that which a particle would have in the $p^+ \rightarrow \infty$ limit (see Ref. 5). We supplement these rules with the observation that the numerator structure of an off-shell spinor line may be written

$$\not{k} + m = \frac{k^+}{p^+} \sum_\lambda \frac{u_\lambda(\vec{k})}{(k^+/p^+)^{1/2}} \frac{u_\lambda(\vec{k})}{(k^+/p^+)^{1/2}} + (k^2 - m^2) \frac{\gamma^+}{2k^+} \quad (2.8)$$

TABLE I. $p_{\mu\nu}(k)$.

$\frac{\hat{\gamma}}{ k}$	=	$\frac{\check{\gamma}}{\hat{\gamma}}$	= $\frac{1}{2}$
$\frac{\hat{\gamma}(v)}{\gamma^+}$	=	$-\frac{1}{2} \frac{v(\wedge)k}{k^+}$	
$\frac{\gamma^+}{\gamma^+}$	=	$\frac{k^-}{k^+}$	
all others = 0			

TABLE II. Matrix elements of one and three γ matrices. $\alpha, \beta =$ helicity in $p^+ \rightarrow \infty$ frame.



	Overall factor	$\alpha = \beta = +$	$\alpha = \beta = -$	$\alpha = +, \beta = -$	$\alpha = -, \beta = +$
$\alpha \xrightarrow{q} \xrightarrow{+} \xrightarrow{k} \beta$	$2p^+$	1	1	0	0
$\alpha \xrightarrow{q} \xrightarrow{-} \xrightarrow{k} \beta$	$\frac{2p^+}{k^+q^+}$	$\hat{q}\check{k} + m^2$	$\hat{k}\check{q}q + m^2$	$-m(\hat{k} - \hat{q})$	$+m(\check{k} - \check{q})$
$\alpha \xrightarrow{q} \xrightarrow{\wedge} \xrightarrow{k} \beta$	$2p^+$	\hat{q}/q^+	\hat{k}/k^+	0	$m \left[\frac{1}{q^+} - \frac{1}{k^+} \right]$
$\alpha \xrightarrow{q} \xrightarrow{V} \xrightarrow{k} \beta$	$2p^+$	\check{k}/k^+	\check{q}/q^+	$-m \left[\frac{1}{q^+} - \frac{1}{k^+} \right]$	0
$\alpha \xrightarrow{q} \xrightarrow{V} \xrightarrow{+} \xrightarrow{\wedge} \xrightarrow{k} \beta$	$8p^+$	1	0	0	0
$\alpha \xrightarrow{q} \xrightarrow{\wedge} \xrightarrow{+} \xrightarrow{V} \xrightarrow{k} \beta$	$8p^+$	0	1	0	0
$\alpha \xrightarrow{q} \xrightarrow{\wedge} \xrightarrow{+} \xrightarrow{-} \xrightarrow{k} \beta$	$8p^+$	0	\hat{k}/k^+	0	$-m/k^+$
$\alpha \xrightarrow{q} \xrightarrow{V} \xrightarrow{+} \xrightarrow{-} \xrightarrow{k} \beta$	$8p^+$	\check{k}/k^+	0	m/k^+	0
$\alpha \xrightarrow{q} \xrightarrow{-} \xrightarrow{+} \xrightarrow{\wedge} \xrightarrow{k} \beta$	$8p^+$	\hat{q}/q^+	0	0	m/q^+
$\alpha \xrightarrow{q} \xrightarrow{-} \xrightarrow{+} \xrightarrow{V} \xrightarrow{k} \beta$	$8p^+$	0	\check{q}/q^+	$-m/q^+$	0
$\alpha \xleftarrow{q} \xrightarrow{\mu} \xrightarrow{k} \beta = \alpha \xrightarrow{q} \xrightarrow{\mu} \xrightarrow{k} \beta$					
$\alpha \xleftarrow{q} \xrightarrow{\mu} \xrightarrow{\nu} \xrightarrow{\lambda} \xrightarrow{k} \beta = \alpha \xrightarrow{q} \xrightarrow{\mu} \xrightarrow{\nu} \xrightarrow{\lambda} \xrightarrow{k} \beta$					

with a similar rule for antifermions. Graphically

$$\longrightarrow = \begin{array}{c} | \\ \hline \longrightarrow \end{array} + \begin{array}{c} \longrightarrow \\ \hline | \end{array} \quad (2.9)$$

Here the spinors are on-shell spinors. The k^- component is placed on shell and the γ^+ term of (2.8) compensates for this correction. Note that this trick combined with the axial gauge of Table I implies that only + and transverse matrix elements need ever be considered for W^{++} , for W^{--} a limited number of - elements are required.

One finds that the amplitudes have the form

$$A^+ \sim a^+(1-x) + b^+/Q + \frac{c^+}{Q^2(1-x)}, \quad (2.10)$$

$$A^- \sim a^-Q$$

up to subleading terms in $(1-x)^{-1}$. The numerator algebra for nonflip contributions appears in Table III. We, of course, only retain those contributions capable of contributing to the leading terms as $x \rightarrow 1$. The phase-space δ function has the expansion

$$\begin{aligned} \delta(x-x_{Bj}) - \delta'(x-x_{Bj}) \frac{2\vec{k}_T \cdot \vec{q}_T}{Q^2} \\ - \delta''(x-x_{Bj}) \frac{m^2 + k_T^2}{Q^2(1-x)} \\ + \frac{1}{2!} \delta'''(x-x_{Bj}) \left[\frac{2\vec{k}_T \cdot \vec{q}_T}{Q^2} \right]^2. \end{aligned} \quad (2.11)$$

We square the amplitude (2.10), multiply by the expansion (2.11), and collect all terms of given powers in $1/Q$ and $1/(1-x)$. [Observe that the derivatives of $\delta(x-x_{Bj})$ lead to extra inverse powers of $(1-x)$.] The resulting forms are

$$\nu W_2 \underset{x \rightarrow 1}{\sim} (1-x)^2 + \text{constant}/Q^2, \quad (2.12)$$

$$\nu W_2 \underset{x \rightarrow 1}{\sim} \text{constant}.$$

More generally (Appendix A) one can show that the leading terms for n -body fermion Fock states behave as⁷

$$\nu W_2 \underset{x \rightarrow 1}{\sim} (1-x)^{2n-3+2|\Delta\lambda|}, \quad (2.13)$$

where $\Delta\lambda$ is the helicity of the initial target spin state minus the helicity of the quark (or antiquark) probed by the virtual photon. The corresponding rule for W_L is

$$\nu W_L \underset{x \rightarrow 1}{\sim} (1-x)^{2n-4+2\Lambda_T}, \quad (2.14)$$

where Λ_T is the helicity of the initial target spin state.

We now discuss the details required to obtain the full result including normalization and spin-flip terms. The color wave function (2.6') and coupling constants yield a factor of $-g_s^2 C_F$. In addition, we convolute with the initial wave function and sum over spin configurations [see (2.6'')]. We define

$$I_A = \int \frac{\phi(\alpha, "Q^{2''})}{\alpha} d\alpha = \frac{f_\pi}{2} \frac{3}{\sqrt{n_c}}, \quad (2.15)$$

$$I_B = \int \frac{\phi(\alpha, "Q^{2''})}{\alpha^2} d\alpha = 2I_A,$$

where the rightmost equalities hold for the form of the wave function given in (2.6). These are the only two independent wave-function weightings which appear once the symmetry under $\alpha \leftrightarrow (1-\alpha)$ of $\phi(\alpha)$ is employed. Denoting, for example, $A_{+-,+}$ as the amplitude for an initial $+-$ helicity to absorb a photon and yield a final $+-$ helicity state, we define amplitudes for fixed final helicity states as

$$\begin{aligned} A_{+-} &= \frac{1}{\sqrt{2}} (A_{+-,+} - A_{-+,-}), \\ A_{++} &= \frac{1}{\sqrt{2}} (A_{+-,++} - A_{-+,++}), \\ A_{-+} &= \frac{1}{\sqrt{2}} (A_{+-,-+} - A_{-+,-+}), \\ A_{--} &= \frac{1}{\sqrt{2}} (A_{+-,--} - A_{-+,-}), \end{aligned} \quad (2.16)$$

corresponding to the coherent helicity-0 initial pion state. We obtain (taking the charge of the struck quark to be unity for the moment)

TABLE III. Numerator γ -matrix algebra results.

A^+ contributions	
	$\underset{x \rightarrow 1}{\sim} \frac{4p^+ k_T^2}{(1-x)\alpha}$
	$\underset{x \rightarrow 1}{\sim} -\frac{4p^+(1-\alpha)\check{q}\hat{k}}{(1-x)}$
	$\underset{x \rightarrow 1}{\sim} -\frac{8p^+ k_T^2}{\alpha(1-x)}$
	$\underset{x \rightarrow 1}{\sim} -\frac{4p^+ k_T^2}{(1-x)}$
A^- contributions	
	$\underset{x \rightarrow 1}{\sim} \frac{4k_T^2}{p^+(1-x)^2} \check{q}\hat{k}$

$\mp \rightarrow \bar{\mp} = \pm \rightarrow \pm$ for all the above

$$\begin{aligned}
 A_{+-}^+ &\underset{x \rightarrow 1}{\sim} \frac{1}{\sqrt{2}} (-C_F \alpha_s 4\pi) \frac{4p^+(1-x)}{(m^2+k_T^2)^2} \left[-(I_A+I_B) - \frac{m^2 I_B}{(k_T^2+m^2)} - \frac{\check{q}\hat{k}}{Q^2(1-x)} (I_B-I_A) \right], \\
 A_{-+}^+ &\underset{x \rightarrow 1}{\sim} -(A_{+-}^+)^*, \\
 A_{++}^+ &\underset{x \rightarrow 1}{\sim} \frac{1}{\sqrt{2}} (-C_F \alpha_s 4\pi) \frac{4p^+(1-x)}{(m^2+k_T^2)^2} \left[\frac{m\check{k}(I_B)}{(m^2+k_T^2)} - \frac{m\check{q}}{Q^2(1-x)} (I_B-I_A) \right], \\
 A_{--}^+ &\underset{x \rightarrow 1}{\sim} +(A_{++}^+)^*, \\
 A_{+-}^- &\underset{x \rightarrow 1}{\sim} \frac{1}{\sqrt{2}} (-C_F \alpha_s 4\pi) \left[\frac{4}{p^+} \right] \left[\frac{\check{q}\hat{k}I_A}{(m^2+k_T^2)} \right] = -(A_{-+}^-)^*, \\
 A_{++}^- &\underset{x \rightarrow 1}{\sim} \frac{1}{\sqrt{2}} (-C_F \alpha_s 4\pi) \left[\frac{4}{p^+} \right] \left[\frac{\check{q}mI_A}{(m^2+k_T^2)} \right] = +(A_{--}^-)^*.
 \end{aligned} \tag{2.17}$$

Note that no terms of the form c^+ in Eq. (2.10) appear. We next square and incorporate final-state phase space; see (1.9) and (1.10). We obtain, using the expansion (2.11),

$$\begin{aligned}
 \nu W_2 &= \frac{\nu}{4\pi} \int d\Gamma^{(2)} \left| \frac{A^+}{p^+} \right|^2 \\
 &\underset{x_{Bj} \rightarrow 1}{\sim} 4C_F^2 \int dk_T^2 \alpha_s^2 \left\{ \frac{1}{(k_T^2+m^2)^2} \left[(I_A+I_B)^2 + \frac{m^2}{(k_T^2+m^2)} (3I_B^2+2I_A I_B) \right] (1-x_{Bj})^2 \right. \\
 &\quad \left. + \frac{1}{Q^2} \frac{1}{(k_T^2+m^2)} \left[4I_A^2 - \frac{m^2}{(k_T^2+m^2)} \left[(3I_B^2-4I_A^2-2I_A I_B) + \frac{(6I_B^2+4I_A I_B)m^2}{k_T^2+m^2} \right] \right] \right\}
 \end{aligned} \tag{2.18}$$

and

$$\begin{aligned}
 \nu W_L &= \frac{Q^2}{4\nu} \frac{1}{4\pi} \int d\Gamma^{(2)} |p^+ A^-|^2 \\
 &\underset{x_{Bj} \rightarrow 1}{\sim} 4C_F^2 \int \frac{dk_T^2 \alpha_s^2}{(m^2+k_T^2)} I_A^2.
 \end{aligned} \tag{2.19}$$

The simplified results of Berger and Brodsky (Ref. 4),

$$\begin{aligned}
 \nu W_2 &\underset{x_{Bj} \rightarrow 1}{\sim} 36C_F^2 I_A^2 \int_{m^2} \frac{dk_T^2}{k_T^4} \alpha_s^2 \left[(1-x_{Bj})^2 + \frac{4}{9} \frac{k_T^2}{Q^2} \right] \\
 &\propto (\sigma_L + \sigma_T),
 \end{aligned} \tag{2.20}$$

$$\nu W_L \underset{x_{Bj} \rightarrow 1}{\sim} 4C_F^2 I_A^2 \int_{m^2} \frac{dk_T^2}{k_T^2} \alpha_s^2 \propto \frac{Q^2}{4x_{Bj}^2} \sigma_L,$$

are obtained by neglecting m^2 's except as an integration cutoff and by using $I_B=2I_A$ as appropriate for the wave function (2.6). In this approximation the higher-twist contribution to νW_2 (proportional to $1/Q^2$) is purely longitudinal. We will see that evaluation of the more general expressions (2.18) and (2.19) does not yield this result until x_{Bj} is very near 1; the longitudinal content of the $1/Q^2$ correction to νW_2 is sensitive to the m^2 scale and to the wave function through I_A and I_B . We evaluate the full expressions (2.18) and (2.19) for the approximate wave function (2.6), and employ a moving coupling constant

$$\alpha_s = \alpha_s^{\text{mom}} \left[\alpha \frac{k_T^2+m^2}{(1-x)} \right] \tag{2.21}$$

with $\alpha = \frac{1}{2}$ for (2.6); α_s is thus the two-loop momentum-subtracted moving coupling evaluated at the off-shell momentum carried by the gluon in the graphs of Fig. 2. This procedure possibly reduces⁸ the higher-order corrections to these graphs when they are evaluated in axial gauge. Note that the term in νW_2 proportional to

$$(4I_A^2/Q^2)/(k_T^2+m^2)$$

is logarithmically divergent without the moving α_s , whereas the additional higher-twist terms with explicit numerator m^2 powers converge. For x_{Bj} very near 1 this near divergence enhances the first term and leads to a purely longitudinal higher-twist correction. However, for practical x_{Bj} values, the results are very different.

The numerical results are best expressed as a function of the variable

$$\chi = \frac{m^2}{\Lambda_{\text{mom}}^2(1-x_{Bj})}, \tag{2.22}$$

where Λ_{mom}^2 is the QCD scale of α_s in (2.21). Defining

$$\begin{aligned}
 \nu W_2^\pi &\underset{x_{Bj} \rightarrow 1}{\sim} (1-x_{Bj})^2 S_s^\pi + \frac{1}{Q^2} T_2^\pi \equiv \nu W_2^{\text{LT}} + \nu W_2^{\text{HT}}, \\
 \nu W_L^\pi &\underset{x_{Bj} \rightarrow 1}{\sim} S_L^\pi
 \end{aligned} \tag{2.23}$$

(LT = leading twist, HT = higher twist), we note that the quantities $m^2 S_2^\pi$, S_L^π , and T_2^π are independent of m^2 at fixed χ . In Fig. 3 we plot, for unit quark charge, $m^2 S_2^\pi$, $T_2^\pi/m^2 S_2^\pi$, and $\langle k_T^2 \rangle/m^2$, where $\langle k_T^2 \rangle$ is defined with respect to the integrand of Eq. (2.18).

The graph begins at $\chi \geq 10$ where the perturbative calculation becomes valid. First it is necessary to comment on the normalization of S_2^π . Data at large x_{Bj} may be extracted from pion-nucleon Drell-Yan pair production using the deep-inelastic determination of the nucleon structure function.⁹ This indirect extraction uses a K factor of 2. The $(1-x_{Bj})^2$ fits to νW_2^{LT} yield an approximate coefficient

$$S_2 = \frac{\nu W_2^{LT}}{(1-x_{Bj})^2} \Big|_{x_{Bj}=0.9} \sim 10 \text{ to } 15. \quad (2.24)$$

From Fig. 3 (corrected for charge-squared factor of $\frac{5}{9}$) we see that an $m^2/\Lambda_{\text{mom}}^2$ value of roughly

$$\frac{m^2}{\Lambda_{\text{mom}}^2} = 1, \quad (2.25)$$

corresponding to $\chi = 10$ at $x_{Bj} = 0.9$ is required to obtain (2.24). For $\Lambda_{\text{mom}} = 0.1$ GeV, in rough agreement with recent determinations,^{1,2,10} we obtain $m^2 = 0.01$ GeV².

To interpret this m^2 value it is helpful to calculate the average transverse momentum squared of the struck quark, $\langle k_T^2 \rangle$. It varies slowly with x_{Bj} as shown in Fig. 3. For example,

$$\langle k_T^2 \rangle = \begin{cases} 1.6m^2, & \chi = 10, \\ 3.3m^2, & \chi = 400. \end{cases} \quad (2.26)$$

Thus $m^2 = 0.01$ GeV² corresponds to an intrinsic trans-

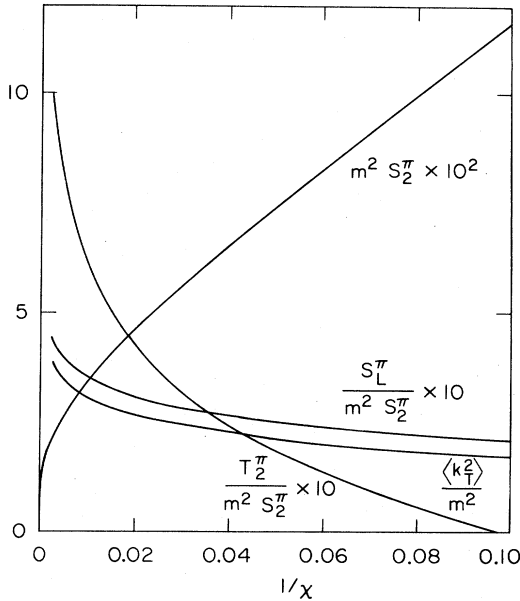


FIG. 3. Results for a "pion" target. Plotted as a function of $\chi = m^2/\Lambda_{\text{mom}}^2(1-x_{Bj})$ are $m^2 S_2^\pi$, $S_L^\pi/m^2 S_2^\pi$, $T_2^\pi/m^2 S_2^\pi$, and $\langle k_T^2 \rangle/m^2$, where $m^2 S_2^\pi$ is in units of (GeV)², all other quantities are dimensionless. Multiply S_2^π by $\sum_q \lambda_q^2$ for a particular type of pion.

verse momentum (at large x_{Bj}) of order 100–200 MeV, well within the conventional phenomenological range. We will discover that this same approximate m^2 value also yields the correct normalization for the nucleon structure function.

From Fig. 3 we see that the normalization of $\nu W_2^{LT}/(1-x_{Bj})^2$ decreases slowly as $x_{Bj} \rightarrow 1$ due to the effects of the moving coupling constant. On the other hand the $1/Q^2$ "higher-twist" component becomes potentially important in precisely this region. From Fig. 3 we see that the predicted values for T_2^π are quite small for $m^2 = 0.01$ GeV². Nonetheless,

$$\frac{\nu W_2^{\text{HT}}}{\nu W_2^{\text{LT}}} = \frac{T_2^\pi}{Q^2 S_2^\pi (1-x_{Bj})^2} \Big|_{Q^2=10 \text{ GeV}^2}^{x_{Bj}=0.99} = 0.5. \quad (2.27)$$

At x_{Bj} values below 0.9, νW_2^{HT} becomes negative but is, in any case, negligible.

The longitudinal structure function νW_L^π is predicted to be independent of x_{Bj} in the limit $x_{Bj} \rightarrow 1$ and will thus also become increasingly important in this region. A useful guide is

$$\frac{\nu W_L}{\nu W_2^{\text{LT}}} \Big|_{m^2=0.01} \sim \begin{cases} 0.2, & x_{Bj}=0.9, \\ 1, & x_{Bj}=0.95. \end{cases} \quad (2.28)$$

Clearly the larger x_{Bj} is the larger Q^2 must be in order for these leading approximations to yield

$$r = \frac{4x_{Bj}^2}{Q^2} \frac{\nu W_L}{\nu W_T} < 1, \quad (2.29)$$

as required by positivity [see Eq. (1.5)].

Our results differ from those of Ref. 4. First our explicit calculations when normalized by comparing to data constrain m^2 to be in a range inconsistent with $\langle k_T^2 \rangle \sim 1$ GeV² as chosen in the first article of Ref. 4. The small m^2 value leads to a small higher-twist coefficient. The exact form of the νW_2^{HT} and W_L calculations, including m^2 numerator algebra contributions, is also more complicated than the Ref. 4 approximation and tends to prevent the higher-twist contribution from being purely longitudinal. Indeed the "transverse" part of νW_2^{HT} is generally negative in our calculation. Only for very small values of $(1-x_{Bj})$ will Eqs. (2.18) and (2.19) yield a purely longitudinal higher-twist component in νW_2 , for it is only by a power of

$$\left[\ln \left(\frac{1}{1-x_{Bj}} \right) \right]^{-1}$$

that the $m^2(k_T^2 + m^2)^{-2}$ contributions are suppressed relative to the $(k_T^2 + m^2)^{-1}$ terms in νW_2^{HT} and νW_L .

The second work quoted in Ref. 4 includes a rough estimate of W_L^π . While their formula for W_L^π is exactly the same as ours, they evaluate it by first relating it to the meson form factor $F_\pi(Q^2)$, and then inputting the phenomenological form determined by low- Q^2 experimental data for F_π . In contrast, in the strict $x_{Bj} \rightarrow 1$ limit, our Eq. (2.19) is equivalent to employing the asymptotic QCD form for the meson form factor. Thus our result

$$W_L^{\pi+} = (0.05 \text{ GeV}^2)^{\frac{5}{9}}/Q^2$$

at $x_{Bj}=0.9$ is approximately a factor of 4 below their estimate, which is probably appropriate at smaller x_{Bj} .

Regarding other possible meson "targets," we note that 0-helicity vector mesons yield exactly the same results as for pions up to an overall normalization factor. Transversely polarized vector mesons exhibit some distinct qualitative differences.

(a) vW_L behaves as $(1-x)^2$ instead of $(1-x)^0$.

(b) vW_2^{HT} receives no matrix-element contributions.

For instance, the diagram of Table III, which is a leading matrix-element higher-twist contribution for the pion-helicity configuration, is zero for a $++\rightarrow++$ helicity configuration. Thus the higher-twist contributions for transversely polarized vector mesons come entirely from the δ -function expansion (2.22) and will yield a negative coefficient.

III. THE PROTON STRUCTURE FUNCTION: PRELIMINARIES

The calculation of the proton structure function proceeds in close analogy to the pion case. However, the number of diagrams for the proton valence three-quark state is much larger. Our classification appears in Fig. 4. The kinematics are illustrated in the A diagrams of Fig. 4. The vectors l and $p-k-l$ are on shell and we define [*in* (+, -, *T*) notation]

$$l = \left[z(1-x)p^+, \frac{l_T^2 + m^2}{z(1-x)p^+}, l_T \right],$$

$$p-k-l = \left[(1-z)(1-x)p^+, \frac{(\vec{l}_T + \vec{k}_T)^2 + m^2}{(1-z)(1-x)p^+}, -(\vec{l}_T + \vec{k}_T) \right], \quad (3.1)$$

$$\vec{L}_T = \vec{l}_T + \vec{k}_T.$$

In this case

$$k^2(x) \underset{x \rightarrow 1}{\sim} -\frac{l_T^2 + m^2}{z(1-x)} - \frac{L_T^2 + m^2}{(1-z)(1-x)} \quad (3.2)$$

is again forced far off-shell and perturbative calculations based on the formalism of Ref. 5 are appropriate. In this region higher Fock states, beyond the valence, are suppressed by powers of $1/k^2(x)$ in the amplitude. We define an evolved wave function for the three-quark state as

$$\phi(\alpha, \beta, "Q^{2}") = \sum_{s_1 s_2 s_3} \int "Q^{2}" \frac{d^2 p_{T1} d^2 p_{T2}}{(16\pi^3)^2} \times \psi_{S_z}(\vec{p}_1 \vec{p}_2 \vec{p}_3 s_1 s_2 s_3) \quad (3.3)$$

with " Q^{2} " set by $1/(1-x_{Bj})$ as in (2.4). At very large " Q^{2} " the form of ϕ for a helicity $+\frac{1}{2}$ proton state,

$$\frac{1}{\sqrt{6}} (2|u^+u^+d^- \rangle - |u^+u^-d^+ \rangle - |u^-u^+d^+ \rangle) + \text{symmetrization} \quad (3.4)$$

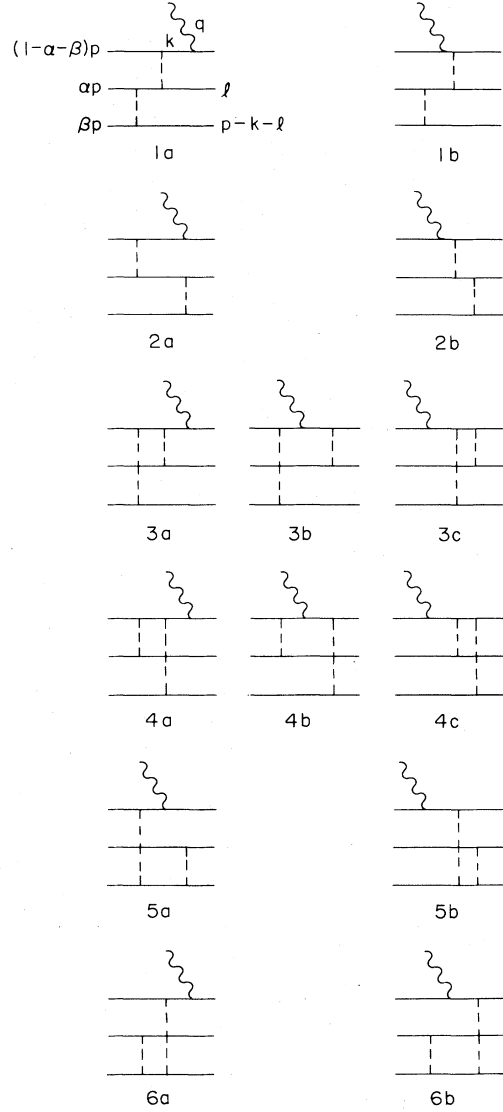


FIG. 4. Enumeration of the tree graphs appropriate at large x_{Bj} for the three-quark valence proton state.

is (neglecting logarithmic structure)

$$\phi(\alpha, \beta, "Q^{2}") \underset{"Q^{2"} \rightarrow \infty}{\sim} C\alpha\beta(1-\alpha-\beta). \quad (3.5)$$

Our calculations, however, are to be compared with data at modest " Q^{2} " values; in this region ϕ is unlikely to have attained its fully evolved form. Other possibilities include a simple weak binding form

$$\phi = B\delta(\alpha - \frac{1}{3})\delta(\beta - \frac{1}{3}). \quad (3.6)$$

A form for ψ based on off-energy-shell dynamics, which leads to good agreement with moderate- Q^2 nucleon form-factor data and $\psi \rightarrow p\bar{p}$ decay, has been proposed by Brodsky, Huang, and Lepage.¹¹

$$\psi_{3q}(\alpha, \beta, \vec{p}_{Ti}) = A \exp \left[-b^2 \left(\frac{p_{T1}^2 + m^2}{(1-\alpha-\beta)} + \frac{p_{T2}^2 + m^2}{\alpha} + \frac{p_{T3}^2 + m^2}{\beta} \right) \right] \quad (3.7)$$

independent of spin. The corresponding ϕ is

$$\begin{aligned} \phi(\alpha, \beta) &= A_\phi \alpha \beta (1-\alpha-\beta) \\ &\times \exp \left[-b^2 m^2 \left(\frac{1}{1-\alpha-\beta} + \frac{1}{\alpha} + \frac{1}{\beta} \right) \right], \end{aligned} \quad (3.8)$$

where the choices

$$A_\phi^2 = 0.35 \text{ GeV}^4, \quad (3.9)$$

$$b^2 m^2 = 0.012 \quad (3.10)$$

yield their best fit. The corresponding valence-state probability is $\leq \frac{1}{4}$. Note that all choices of ϕ are symmetric under $\alpha \leftrightarrow \beta \leftrightarrow 1-\alpha-\beta$. Various integral weightings of ϕ will appear in our diagram evaluations. Those appearing in νW_2^{LT} and νW_L are

$$\begin{aligned} I_A &= \int \phi(\alpha, \beta) d\alpha d\beta \frac{1}{\beta(\alpha+\beta)^2}, \\ I_B &= \int \phi(\alpha, \beta) d\alpha d\beta \frac{1}{\alpha\beta(1-\alpha)}, \\ I_C &= \int \phi(\alpha, \beta) d\alpha d\beta \frac{1}{\beta^2(\alpha+\beta)}, \\ I_D &= \int \phi(\alpha, \beta) d\alpha d\beta \frac{1}{\alpha\beta^2}. \end{aligned} \quad (3.11)$$

In comparing results for different wave functions, we normalize B and C of Eqs. (3.5) and (3.6) so that the I_A values for these wave functions are the same as for (3.8). Since the I_A weighting dominates the nucleon-form-factor calculation, this will lead to the same form-factor normalization for all three cases.

As in the pion calculations the moving coupling constants will be evaluated at the momentum transfer carried by the associated gluon. The wave-function momentum fractions α , β or $\gamma = \alpha + \beta$ appear in these arguments and are evaluated at their average values for the particular type of integral I_A, \dots, I_D which weights a given contribution. We denote these average values by

$$\langle \alpha \rangle_{I_A}, \langle \beta \rangle_{I_A}, \langle \gamma \rangle_{I_A}, \text{ etc.}$$

The color wave function for the proton is taken as (normalized to unity)

$$\frac{1}{\sqrt{6}} \epsilon_{abc}, \quad (3.12)$$

which yields a color factor of

$$\text{color factor} = \frac{4}{9} = \frac{1}{3} C_F \quad (3.13)$$

for each amplitude diagram of Fig. 4. Note also that the tree graph involving the three-gluon vertex is zero for the color wave function of (3.12).

We are now ready to discuss amplitude evaluations. For the moment we consider only terms with leading $x \rightarrow 1$ behavior in a given order of $1/Q$. For νW_2 we list those forms capable of yielding

$$\nu W_2 \sim \begin{cases} (1-x)^3, \\ (1-x)/Q^2, \\ 1/Q^4(1-x), \end{cases} \quad (3.14)$$

while for νW_L we will only keep terms contributing in order $1/Q^0$ (i.e., to σ_L/σ_T in order $1/Q^2$)

$$\nu W_L \sim (1-x)^3. \quad (3.15)$$

These are

$$\begin{aligned} A^+ &\underset{x \rightarrow 1}{\sim} a^+(1-x) + \frac{b^+}{Q} + \frac{c^+}{[Q^2(1-x)]} \\ &\quad + \frac{d^+}{Q^3(1-x)^2} + \frac{e^+}{Q^4(1-x)^3}, \\ A^- &\underset{x \rightarrow 1}{\sim} a^-(1-x)Q. \end{aligned} \quad (3.16)$$

Final-state phase space provides one power of $(1-x)$, so that upon computing $(1-x) |A|^2$ we obtain

$$\begin{aligned} \nu W_2 &\underset{x \rightarrow 1}{\propto} a^{+2}(1-x)^3 + \dots, \\ \nu W_L &\underset{x \rightarrow 1}{\propto} a^{-2}(1-x)^3, \end{aligned} \quad (3.17)$$

in agreement with (2.13) and (2.14).

IV. νW_2

The results for A^+ are easily summarized. First, the possible power-suppressed corrections, with leading $x_{\text{Bj}} \rightarrow 1$ behavior listed in (3.16), to the dominant a^+ term do not arise; i.e., $b^+ = c^+ = d^+ = e^+ = 0$. There are numerous terms contributing to A^+ of order

$$A_{\text{nonleading}}^+ \underset{x \rightarrow 1}{\sim} \frac{(1-x)}{Q}, \frac{1}{Q^2}, \dots, \quad (4.1)$$

but those are not as important in the strict $x_{\text{Bj}} \rightarrow 1$ limit of νW_2 as the various $1/Q^2$ and $1/Q^4$ corrections arising purely from the expansion of the $-$ component momentum-conservation phase-space δ function. We refer to this as the absence of leading higher-twist "matrix-element" contributions in the $x_{\text{Bj}} \rightarrow 1$ limit. This absence is related to the extra power of $(1-x)$ in A^- relative to the pion calculation [compare (3.16) to (2.10)], which in turn arises from the nonzero helicity of the incident photon. However, terms of the form (4.1) will be computed later and will be found to be phenomenologically more important than the terms we consider now.

In the gauge (2.7), only a very few diagrams contribute to the a^+ term of Eq. (3.16). The Feynman-graph-numerator results for the nonzero γ -matrix configurations are listed in Table IV for the nonflip helicity configuration $+-+ \rightarrow +-+$.

We have defined the variables

$$T = \frac{l_T^2 + m^2}{z}, \quad U = \frac{L_T^2 + m^2}{(1-z)}, \quad S = U + T. \quad (4.2)$$

TABLE IV. Numerator results. A^+ nonflip contributions (charge and color factors omitted).

$$\begin{aligned}
 & \begin{array}{c} + \\ | \\ + \\ | \\ + \\ | \\ + \end{array} \xrightarrow{x \rightarrow 1} - \frac{16p^+}{(1-x)^3} \frac{\beta}{\alpha+\beta} \frac{S\hat{L}\check{L}}{z(1-z)} \\
 & \begin{array}{c} + \\ | \\ + \\ | \\ + \\ | \\ + \end{array} \xrightarrow{x \rightarrow 1} - \frac{16p^+}{(1-x)^3} \frac{\alpha}{\alpha+\beta} \frac{S\check{L}\hat{L}}{z(1-z)} \\
 & \begin{array}{c} + \\ | \\ + \\ | \\ + \\ | \\ + \end{array} \xrightarrow{x \rightarrow 1} + \frac{8p^+}{(1-x)^3} \frac{T\hat{L}\check{L}}{z(1-z)}
 \end{aligned}$$

Only diagrams 2A, 5A, and 4A of Fig. 4 contribute as $x \rightarrow 1$. The corresponding denominator products are

$$\begin{aligned}
 (d_{2A}) &= \frac{(1-x)^4}{\beta^2(\alpha+\beta)US^3}, \\
 (d_{5A}) &= \frac{(1-x)^4}{\alpha^2(\alpha+\beta)TS^3}, \\
 (d_{4A}) &= \frac{(1-x)^4}{\alpha\beta(1-\beta)UT^2S}.
 \end{aligned} \tag{4.3}$$

The moving coupling constants appearing in the various diagrams are evaluated at the average off-shell momentum transfers carried by the two gluons. The absolute values of these momenta transfers are

$$\begin{aligned}
 A_{+-+}^+ &\sim \frac{1}{\sqrt{6}} (cA_{+-+,++-}^+ + dA_{+-+,++-}^+) = \frac{1}{\sqrt{6}} A (c\check{L}\hat{L} + dm^2), \\
 A_{-+-}^+ &\sim \frac{1}{\sqrt{6}} (cA_{-+-,++-}^+ + dA_{-+-,++-}^+) = \frac{1}{\sqrt{6}} A (cm^2 + d\check{L}\hat{L}), \\
 A_{+--}^+ &\sim \frac{1}{\sqrt{6}} (cA_{+--,++-}^+ + dA_{+--,++-}^+) = \frac{1}{\sqrt{6}} A (cm\hat{L} - dm\check{L}), \\
 A_{+++}^+ &\sim \frac{1}{\sqrt{6}} (cA_{+++}^+ + dA_{+++}^+) = \frac{1}{\sqrt{6}} A (cm\check{L} - dm\hat{L}),
 \end{aligned} \tag{4.7}$$

$$2A: \frac{(\alpha+\beta)S}{(1-x)}, \frac{BU}{(1-x)},$$

$$5A: \frac{(\alpha+\beta)S}{(1-x)}, \frac{\alpha t}{(1-x)}, \tag{4.4}$$

$$4A: \frac{\alpha T}{(1-x)}, \frac{\beta U}{(1-x)}.$$

Combining Table IV, Eqs. (3.11), (3.13), (4.3), and (4.4), and using $\alpha \leftrightarrow \beta$ symmetry of ϕ , we obtain

$$\begin{aligned}
 A_{+-+,++-}^+ &\xrightarrow{x \rightarrow 1} -8p^+(1-x) \left(\frac{1}{3}C_F\right) (4\pi)^2 \frac{\hat{L}\check{L}}{z(1-z)} \\
 &\quad \times \left[2I_A \left[\frac{(\gamma AS)(\beta AU)}{US^2} + \frac{(\gamma AS)(\beta AT)}{TS^2} \right] \right. \\
 &\quad \left. - I_B \frac{(\beta BT)(\alpha BU)}{UTS} \right] \\
 &\equiv A\hat{L}\check{L}.
 \end{aligned} \tag{4.5}$$

We have introduced the notation (defining $\gamma \equiv \alpha + \beta$)

$$\begin{aligned}
 (\gamma AS) &\equiv \alpha_s [\langle \alpha + \beta \rangle_{I_A} S / (1-x)], \\
 (\alpha BU) &\equiv \alpha_s [\langle \alpha \rangle_{I_B} U / (1-x)], \\
 (\beta CU) &\equiv \alpha_s [\langle \beta \rangle_{I_C} U / (1-x)],
 \end{aligned} \tag{4.6}$$

etc.

At this point note that A vanishes if the weak-binding wave function (3.6), which implies $I_B = 2I_A$, is chosen and if the α_s 's are taken to be constant.

The leading helicity-flip contributions are easily summarized. First, the upper line may not flip without losing a power of $(1-x)$ [see Eq. (2.13)]. Helicity flip for the middle line leads to the replacement in Eq. (4.5) of \hat{L} by $(-m)$. Helicity flip for the lower line leads to $\check{L} \rightarrow -m$. Helicity flip for both lines results in $\hat{L}\check{L} \rightarrow m^2$.

The results for initial helicity configuration $+-+$ are obtained from the above by $T \leftrightarrow U$, $\alpha \leftrightarrow \beta$, and $\vec{L}_T \rightarrow -\vec{L}_T$ interchange which leaves A in (4.5) unchanged. The initial $-+-$ helicity configuration does not contribute to the leading $x \rightarrow 1$ behavior.

For the spin wave function (3.4) we thus obtain the final-state spin amplitudes

leading to

$$|M|^2 \equiv |A_{+-+}^+|^2 + |A_{+--}^+|^2 + |A_{-+-}^+|^2 + |A_{--+}^+|^2 \\ = A^2 \frac{(c^2 + d^2)}{6} (l_T^2 + m^2)(L_T^2 + m^2). \quad (4.8)$$

For a proton, Eq. (3.4) implies that for each struck u quark (of $+$ helicity)

$$c = 2, \quad d = -1, \quad (4.9a)$$

while for the struck d quark (of $+$ helicity)

$$c = -1, \quad d = -1. \quad (4.9b)$$

The above does not include the charge-squared factor. Using the weightings (4.9) we obtain (after including the charge factors)

$$|M|_{\text{proton}}^2 = |A|^2 \left(\frac{7}{9}\right) (l_T^2 + m^2)(L_T^2 + m^2). \quad (4.10)$$

For a neutron target the $\frac{7}{9}$ is replaced by a $\frac{3}{9}$ yielding the well-known $\frac{3}{7}$ ratio for $(\nu W_2^{\text{LT}})_{\text{neutron}} / (\nu W_2^{\text{LT}})_{\text{proton}}$.¹²

Note that the helicity-flip terms in net, merely change

the helicity-nonflip factor $l_T^2 L_T^2$, which would have appeared in (4.10) to $(l_T^2 + m^2)(L_T^2 + m^2)$. This is, of course, much simpler than what happens in the pion case. This simplicity is quickly traced to the fact that the line struck by the photon cannot flip helicity in the proton case [without extra $(1-x)$ suppression], whereas it may in the pion case.

The final-state phase-space factor for the proton three-quark Fock state is $d\Gamma^{(3)}$, given in (1.9). We have

$$d\Gamma^{(3)} = \sum_{\text{final helicities}} \frac{d^2 l_T d^2 L_T (1-x) dz dx}{(16\pi^3)^2} \\ \times 2\pi \delta \left[2\nu - \frac{S}{1-x} - \frac{(\vec{k}_T + \vec{q}_T)^2 + m^2}{x} \right]. \quad (4.11)$$

As before, we will expand the δ function, this time up to order $1/Q^4$. Because the matrix element $|M|^2$ is even under both $\vec{l}_T \rightarrow -\vec{l}_T$ and $\vec{L}_T \rightarrow -\vec{L}_T$, we can use the simplified form

$$d\Gamma^{(3)} \underset{x_{\text{Bj}} \rightarrow 1}{\sim} \frac{\pi}{\nu} \sum_{\text{final helicity states}} \int \frac{dx dz (1-x) \pi dL_T^2 \pi dl_T^2}{(16\pi^3)^2} \\ \times \left[\delta(x - x_{\text{Bj}}) - \frac{S}{Q^2(1-x)} \delta'(x - x_{\text{Bj}}) + \left[\frac{L_T^2 + l_T^2}{Q^2} + \frac{1}{2} \frac{S^2}{Q^4(1-x)^2} \right] \delta''(x - x_{\text{Bj}}) \right. \\ \left. - \frac{(L_T^2 + l_T^2)S}{Q^4(1-x)} \delta'''(x - x_{\text{Bj}}) + \frac{1}{4} \frac{(L_T^4 + l_T^4 + 4L_T^2 l_T^2)}{Q^4} \delta''''(x - x_{\text{Bj}}) + \mathcal{O} \left[\frac{1}{Q^6} \right] \right]. \quad (4.12)$$

We finally obtain νW_2 as

$$\nu W_2 = \frac{\nu}{4\pi} \int d\Gamma^{(3)} \left| \frac{A^+}{p^+} \right|^2. \quad (4.13)$$

First let us examine the x integral. The important x dependence in (4.13) is a series of terms of the form

$$I(x_{\text{Bj}}) \equiv \int dx (1-x)^3 \alpha_s \left[\frac{C_1}{1-x} \right] \alpha_s \left[\frac{C_2}{1-x} \right] \alpha_s \left[\frac{C_3}{1-x} \right] \alpha_s \left[\frac{C_4}{1-x} \right] \\ \times \left[\delta(x - x_{\text{Bj}}) - \frac{S}{Q^2(1-x)} \delta'(x - x_{\text{Bj}}) + \left[\frac{L_T^2 + l_T^2}{Q^2} + \frac{S^2}{Q^4(1-x)^2} \right] \delta''(x - x_{\text{Bj}}) \right. \\ \left. - \frac{(L_T^2 + l_T^2)S}{Q^4(1-x)} \delta'''(x - x_{\text{Bj}}) + \frac{1}{4} \left[\frac{(L_T^4 + 4L_T^2 l_T^2 + l_T^4)}{Q^4} \delta''''(x - x_{\text{Bj}}) \right] \right]. \quad (4.14)$$

We note that for

$$\alpha_s \equiv \frac{a}{\ln \left[\frac{c}{1-x} \right]}, \quad a = \frac{4\pi}{11 - \frac{2}{3}\eta_F}, \quad (4.15)$$

we have

$$\alpha'_s = \frac{d\alpha_s}{dx} = -\frac{\alpha_s^2}{a(1-x)}. \quad (4.16)$$

The $1/Q^2$ correction terms which involve $\int (1-x)^2 \delta'(x-x_{Bj})$ and $\int (1-x)^3 \delta''(x-x_{Bj})$ receive their leading contribution by differentiating the explicit $(1-x)$ power the maximal number of times. Contributions obtained by differentiating one of the α_s 's are suppressed by a single α_s relative to these leading contributions. In contrast, the $1/Q^4$ correction terms involve integrals of the form

$$\int (1-x) \delta''(x-x_{Bj}), \quad \int (1-x)^2 \delta'''(x-x_{Bj}), \quad \text{or} \quad \int (1-x)^3 \delta''''(x-x_{Bj}),$$

which would be zero unless one of the δ -function derivatives is partially integrated against a moving coupling α_s . Thus the leading $1/Q^4$ term will involve an integral over five powers of α_s , versus four. Defining

$$\Sigma(\alpha_s) = \sum_{i=1}^4 \alpha_s \left[\frac{C_i}{1-x} \right], \quad \Pi(\alpha_s) = \prod_{i=1}^4 \alpha_s \left[\frac{C_i}{1-x} \right], \quad (4.17)$$

Eq. (4.14) reduces to

$$I(x_{Bj}) = (1-x_{Bj})^3 \Pi(\alpha_s) \Big|_{x=x_{Bj}} + \frac{(1-x_{Bj})}{Q^2} [6(L_T^2 + l_T^2) - 2S] \Pi(\alpha_s) \Big|_{x=x_{Bj}} \\ + \frac{1}{aQ^4(1-x_{Bj})} \left[\frac{S^2}{2} - 2(L_T^2 + l_T^2)S + \frac{6(L_T^4 + l_T^4 + 4L_T^2 l_T^2)}{4} \right] [\Pi(\alpha_s) \Sigma(\alpha_s)] \Big|_{x=x_{Bj}}. \quad (4.18)$$

Writing the leading power-law contributions as

$$\nu W_2 \Big|_{x_{Bj} \rightarrow 1} \sim S_2 (1-x_{Bj})^3 + \frac{T_2}{Q^2} (1-x_{Bj}) + \frac{U_2}{Q^4 (1-x_{Bj})} + \dots, \quad (4.19)$$

we obtain the following explicit expression for S_2^{proton} from (4.13), (4.5), (4.10), and (4.12):

$$S_2^g = 2^4 \left(\frac{7}{9}\right) \left(\frac{1}{3} C_F\right)^2 \int_0^1 dz \int_{m^2/z}^\infty T dT \int_{m^2/1-z}^\infty U dU \left[2I_A \left[\frac{(\gamma AS)(\beta AU)}{US^2} + \frac{(\gamma AS)(\beta AT)}{TS^2} \right] - I_B \frac{(\beta BT)(\alpha BU)}{UTS} \right]^2. \quad (4.20)$$

The expression for T_2 is easily obtained, following the procedure just outlined in (4.18) by multiplying the integrand of (4.20) by

$$\{6[U(1-z) + Tz - 2m^2] - 2S\}.$$

The expression for U_2 is similarly obtained by following the procedure of (4.18). It is clear that U_2 vanishes unless we employ moving coupling constants. That this is also true of T_2 is less obvious; nonetheless it can be verified by analytic calculation that T_2 is indeed identically zero for constants α_s . Thus both T_2 and U_2 are sensitive to the manner in which we have approximated higher-order corrections to our tree graphs through evaluating the moving coupling constants as specified in Eq. (2.26). For constant α_s the leading power-law corrections to νW_2 behave as $(1-x)^2/Q^2$ and $1/Q^4$, thus establishing contact with the results of Ref. 13; see Appendix B for further comparison.

Our complete results are easily summarized. First we note that the ratios T_2/S_2 and U_2/S_2 are very insensitive to the wave-function choice. Only the normalization of S_2 exhibits any sensitivity. For a given choice of m the S_2 normalization values of $\chi = 10$ are in the ratio

$$S_2[\text{Eq. (3.5)}]: S_2[\text{Eq. (3.6)}]: S_2[\text{Eq. (3.8)}] \\ = 0.147:0.022:0.051, \quad (4.21)$$

i.e., the normalization changes by a factor of 7 for different wave-function choices. This sensitivity is due to the tendency for cancellation between the I_A and I_B terms of (4.20). Indeed, for the wave function (3.6), S_2 is identi-

cally zero for constant α_s . We present results for the proton, with wave-function choice (3.6), in Fig. 5. There we plot the m -independent [at fixed χ , see (2.22)] quantity $m^4 S_2^{\text{proton}}$ as a function of χ . The results for T_2/S_2 and U_2/S_2 show that they vary slowly with x_{Bj} , i.e., with χ :

$$\frac{T_2}{S_2} = -m^2 \begin{cases} 7, & \chi = 10, \\ 4, & \chi = 400, \end{cases} \quad (4.22)$$

$$\frac{U_2}{S_2} = m^4 \begin{cases} 70, & \chi = 10, \\ 24, & \chi = 400. \end{cases} \quad (4.23)$$

Results for a neutron target are easily summarized. We find $S_2^n/S_2^g = \frac{3}{7}$ as obtained in Ref. 12, while T_2/S_2 and U_2/S_2 are target independent. The $\frac{3}{7}$ ratio above is, of course, a direct consequence of the fact that only struck quarks with + helicity before and after photon absorption contribute to S_2 [see (4.7)–(4.9)].

In order to determine an approximate m^2 value we (as in the pion case) look at the overall normalization of the leading-twist contribution S_2^{proton} . Data at $\chi_{Bj} > 0.9$ is not available. We adopt the procedure of extrapolating the plots of Fig. 5 to small χ and find that the approximate experimental result

$$\nu W_2^{\text{proton}} \Big|_{x_{Bj} \approx 0.7} \sim 0.5(1-x_{Bj})^3 \quad (4.24)$$

requires

$$m^2 \leq 0.006 \text{ GeV}^2, \quad (4.25)$$

where $\Lambda_{\text{mom}}^2 = 0.01 \text{ GeV}^2$ has again been employed. We

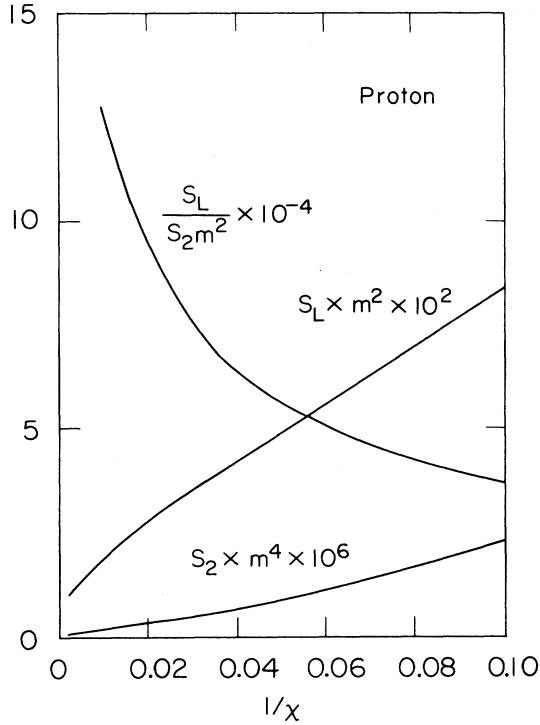


FIG. 5. Results for a proton target. Plotted are $m^4 S_L^2$, $m^2 S_L^2$, and $S_L^2/m^2 S_2^2$ as a function of χ , where $m^4 S_L^2, m^2 S_L^2$ are in units of GeV^4 , while $S_L^2/m^2 S_2^2$ is dimensionless.

note that this is roughly the same size for m^2 as required in the pion case, Eq. (2.24). In fact, for future discussion we will employ $m^2=0.01 \text{ GeV}^2$. Once again we calculate $\langle k_T^2 \rangle$ as a function of m^2 . For the proton we obtain

$$\langle k_T^2 \rangle = \begin{cases} 2.8m^2, & \chi = 10, \\ 3.9m^2, & \chi = 400, \end{cases} \quad (4.26)$$

which, for $m^2 \leq 0.01$, yields a very reasonable intrinsic transverse momentum.

It should be apparent from (4.22), (4.23), and (4.19) that none of the leading corrections to νW_2^{proton} are very sizable for the value $m^2 \leq 0.01$ determined from overall normalization. In a later section we will discuss nonleading corrections to νW_2 of the form given below by V_2 and X_2 :

$$\nu W_2 \underset{x_{\text{Bj}} \rightarrow 1}{\sim} S_2(1-x_{\text{Bj}})^3 + \frac{T_2}{Q^2}(1-x_{\text{Bj}}) + \frac{U_2}{Q^4(1-x_{\text{Bj}})} + V_2(1-x_{\text{Bj}})^4 + X_2 \frac{(1-x_{\text{Bj}})^2}{Q^2} + \dots \quad (4.27)$$

These corrections receive contributions both from explicit matrix elements and from kinematical terms generated through δ function and other expansion corrections to the leading S_2 term. In addition neither V_2 nor X_2 vanishes for constant α_s .

V. νW_L

First, however, let us turn to a discussion of the longitudinal structure function νW_L . For spin- $\frac{1}{2}$ quarks νW_L scales. The determination of νW_L requires computing the amplitude A^- . In this case, as $x_{\text{Bj}} \rightarrow 1$, all three initial helicity configurations $+-+$, $++-$, and $-++$ and all eight final helicity configurations contribute to the behavior

$$\nu W_L \underset{x_{\text{Bj}} \rightarrow 1}{\sim} S_L(1-x_{\text{Bj}})^3.$$

In addition, diagram types 1A, 2A, 3A, 4A, 5A, and 6A all make contributions in axial gauge and most receive contributions from several γ -matrix configurations. [Note that in axial gauge B- and C-type photon attachments (see Fig. 4) do not contribute to the leading $x_{\text{Bj}} \rightarrow 1$ behavior.] It is neither useful nor practical to tabulate in detail all the contributions. Instead we confine ourselves to writing out the amplitude for $+-+ \rightarrow +-+$, $++- \rightarrow ++-$, and $-++ \rightarrow -++$, and then illustrate how to combine these to obtain νW_L . We use the short-hand notation for the α_s 's given in (4.6).

The structures of the nonflip amplitudes for the three possible helicity states are

$$A_{+-+, +-+}^- = A\hat{q}\hat{l} + B\hat{q}\hat{L}\hat{l}\hat{l} \quad (5.1)$$

with $A_{+-+, +-+}^-$ obtained by $\vec{L}_T \leftrightarrow \vec{l}_T$, $z \leftrightarrow (1-z)$, $\alpha \leftrightarrow \beta$ from $A_{+-+, +-+}$, and

$$A_{-++, -++}^- = \bar{A}\hat{q}\hat{l} + \bar{C}\hat{q}\hat{L}\hat{l}. \quad (5.2)$$

We define

$$A = \frac{4(1-x)(4\pi)^2}{p^+z(1-z)} [(1-z)E + L_T^2 H], \quad (5.3)$$

$$B = \frac{4(1-x)(4\pi)^2}{p^+z(1-z)} F$$

and obtain (charge and color factors are omitted)

$$E \underset{x \rightarrow 1}{\sim} \left[\frac{2I_C}{SU}(\beta CU)(\gamma CS) + \frac{I_A}{SU}(\beta AU)(\gamma AS) - \frac{I_C}{S^2} + (\beta CU)(\gamma CS) + \frac{I_B}{TU}(\beta BU)(\alpha BT) - \frac{I_B}{TS}(\beta BU)(\alpha BT) + \frac{2I_D}{TU}(\beta BD)(\alpha DT) + \frac{2I_A}{TS}(\beta AT)(\gamma AS) + \frac{I_C U}{TS^2}(\beta CT)(\gamma CS) + \frac{I_B}{TS}(\beta BT)(\alpha BU) \right], \quad (5.4a)$$

$$F_{x \rightarrow 1} \sim \left[\frac{I_C}{US^2}(\beta CU)(\gamma CS) + \frac{I_A}{US^2}(\beta AU)(\gamma AS) + \frac{I_A}{TS^2}(\beta AT)(\gamma AS) - \frac{I_B}{TUS}(\beta BT)(\alpha BU) \right], \quad (5.4b)$$

$$H_{x \rightarrow 1} \sim \left[\frac{I_A}{U^2S}(\beta AU)(\gamma AS) - \frac{I_C}{US^2}(\beta CU)(\gamma CS) - \frac{2I_A}{US^2}(\beta AU)(\gamma AS) - \frac{I_B}{U^2T}(\alpha BT)(\beta BU) \right. \\ \left. + \frac{I_B}{UTS}(\alpha BT)(\beta BU) - \frac{I_C}{TS^2}(\beta CT)(\gamma CS) - \frac{2I_A}{TS^2}(\beta AT)(\gamma AS) + \frac{I_B}{STU}(\beta BT)(\alpha BU) \right]. \quad (5.4c)$$

For the $-++$ case we define

$$\bar{A} = \frac{4(1-x)(4\pi)^2}{p^+z(1-z)} [(1-z)\bar{E} + L_T^2\bar{H}], \quad \bar{C} = \frac{4(1-x)(4\pi)^2}{p^+z(1-z)} [z\bar{G} + I_T^2\bar{F}], \quad (5.5)$$

and obtain

$$\bar{E} = \left[\frac{2I_C}{SU}(\beta CU)(\gamma CS) + \frac{I_A}{SU}(\beta AU)(\gamma AS) - \frac{I_C}{S^2}(\beta CU)(\gamma CS) + \frac{I_B}{TU}(\beta BU)(\alpha BT) - \frac{I_B}{TS}(\beta BU)(\alpha BT) \right. \\ \left. + \frac{2I_D}{TU}(\beta DU)(\alpha DT) - \frac{2I_C}{TS}(\beta CT)(\gamma CS) + \frac{I_C U}{TS^2}(\beta CT)(\gamma CS) + \frac{I_B}{TS}(\alpha BU)(\beta BT) \right], \quad (5.6a)$$

$$\bar{F} = \left[\frac{I_C}{US^2}(\beta CU)(\gamma CS) + \frac{I_B}{UTS}(\beta BU)(\alpha BT) + \frac{I_A}{T^2S}(\beta AT)(\gamma AS) - \frac{I_C}{TS^2}(\beta CT)(\gamma CS) \right. \\ \left. - \frac{I_B}{UT^2}(\beta BT)(\alpha BU) - \frac{I_B}{UTS}(\beta BT)(\alpha BU) \right], \quad (5.6b)$$

$$\bar{G} = -\bar{E}(T \leftrightarrow U), \quad (5.6c)$$

$$\bar{H} = -\bar{F}(T \leftrightarrow U). \quad (5.6d)$$

The full result for νW_L is obtained, in this helicity-nonflip case, by combining the absolute squares of the amplitudes for the various helicity configurations and charge choices according to the wave-function weighting (3.4) and using (1.4) and (1.10) to obtain

$$\nu W_L = \frac{Q^2}{4\nu} \int d\Gamma^{(3)}(p^+)^2 \frac{|A^-|^2}{4\pi} \\ \sim_{x_{Bj} \rightarrow 1} S_L (1-x_{Bj})^3, \quad (5.7)$$

where, for S_L , we keep only the leading term in $d\Gamma^{(3)}$ of Eq. (4.12).

The result for νW_L^{proton} obtained by keeping only these helicity-nonflip terms was given in Ref. 3 for the wave function (3.8). Helicity-flip terms, which are explicitly proportional to the mass m , are important, however, for all χ values we have considered. They result in a moderate increase in the value of S_L^p . For instance, for the wave function (3.6) we obtain (in units of GeV^4)

$$m^2 S_L^p = \begin{cases} \text{nonflip} & \text{all} \\ 3.3 \times 10^{-2} & 8.3 \times 10^{-2}, \chi=10, \\ 3.7 \times 10^{-3} & 1.0 \times 10^{-2}, \chi=400. \end{cases} \quad (5.8)$$

Our complete answer will include the helicity-flip terms and employ the wave function (3.6). We have investigated the sensitivity of the ratio $S_L^p/m^2 S_L^q$ to the wave-function choice in the helicity-nonflip approximation. We find

only a mild sensitivity throughout the entire χ range. For example,

$$\frac{S_L^p}{m^2 S_L^q} \simeq \begin{matrix} \text{Eq. (3.8)} & \text{Eq. (3.6)} \\ \left\{ \begin{array}{cc} 3.6 \times 10^4 & 1.5 \times 10^4, \chi=10, \\ 4.5 \times 10^4 & 7.9 \times 10^4, \chi=400. \end{array} \right. \end{matrix} \quad (5.9)$$

The complexity of the full result for νW_L (obtained by using REDUCE¹⁴) is apparent in the “invariant-amplitude” expansions of the amplitudes A^- for fixed final helicity states (the coherent sum over initial helicity states having been performed). Each helicity amplitude contains terms proportional to various vector quantities such as \hat{q} , \hat{l} , \hat{L}^2 , etc., as in (5.1) and (5.2). The coefficients of the vector quantities are the invariant amplitudes—there is one invariant amplitude for each vector structure which appears in a given helicity amplitude. We list the vector structures which appear for each amplitude in leading order as $x_{Bj} \rightarrow 1$:

$$A_{+++}^- \propto \hat{q}(1, \hat{L}\hat{l}, \hat{L}\hat{l}), \\ A_{++-}^- \propto \hat{q}(\hat{L}, \hat{l}, \hat{L}^2\hat{l}, \hat{l}^2\hat{L}), \\ A_{+-}^- \propto \hat{q}(\hat{L}, \hat{L}^2, \hat{l}^2), \\ A_{+--}^- \propto \hat{q}(\hat{l}, \hat{L}, \hat{L}^2\hat{l}, \hat{l}^2\hat{L}), \\ A_{-++}^- \propto \hat{q}(\hat{L}, \hat{l}), \quad (5.10)$$

$$A_{-+-}^- \propto \hat{q}(1, \hat{L}\hat{l}, \hat{L}\hat{l}),$$

$$A_{--+}^- \propto \hat{q}(1, \hat{L}\hat{l}, \hat{L}\hat{l}),$$

$$A_{---}^- \propto \hat{q}(\hat{L}, \hat{l}).$$

The invariant amplitudes multiplying these vector structures are, in general, lengthy expressions of which (5.4) and (5.6) are zero-mass reductions. They are, of course, functions of T , U , and z at fixed m and x_{Bj} . We compute the full νW_L from the squares of the above amplitudes using (5.7). We plot $m^2 S_L^p$ as a function of χ in Fig. 5, as well as the ratio $S_L^p/m^2 S_2^p$. We see that at $\chi \lesssim 10$, corresponding for $\Lambda_{\text{mom}}=0.1$ GeV and $m=0.1$ GeV to $x_{\text{Bj}} \leq 0.9$, this ratio is slowly varying with value

$$S_L^p/m^2 S_2^p \simeq 4 \times 10^4. \quad (5.11)$$

For larger χ , x_{Bj} values the ratio increases.

The result corresponding to (5.11) for a neutron target is easily summarized as

$$\frac{S_L^n}{m^2 S_2^n} \approx 2 \frac{S_L^p}{m^2 S_2^p} \quad (5.12)$$

(good to 3% over the range $\chi=10$ to 400) or, using the result

$$\frac{S_2^n}{S_2^p} = \frac{3}{7}, \quad (5.13)$$

we have

$$\frac{S_L^n}{S_L^p} \approx \frac{6}{7}. \quad (5.14)$$

While (5.13) is an exact result, following from the fact that the quark struck by the deep-inelastic photon must have + helicity (for a + helicity proton) both before and after photon absorption in order to contribute to S_2 , (5.14) is not an exact result. Both + and - helicity quarks contribute to S_L and with different amplitudes. In addition there are leading contributions to S_L in which an initially negative-helicity quark is struck by the photon and flips helicity so as to contribute to the same final-state helicity amplitude as an initially positive-helicity struck quark. This results in interference between terms arising from initial quarks of different helicities.

The value (5.11) corresponds to [see Eq. (1.5)]

$$\frac{\sigma_L}{\sigma_T} \Big|_{x_{\text{Bj}}=0.9} \sim 1.6 \times 10^5 \frac{m^2}{Q^2}, \quad (5.15)$$

implying that very large Q^2 values are required before an asymptotic series for this ratio becomes appropriate. We do not see any justification in the large- x_{Bj} region for the usual statement that a small $\langle k_T^2 \rangle$ value guarantees a small value for the $1/Q^2$ coefficient in σ_L/σ_T . While the scale of this $1/Q^2$ coefficient is set by the same quantity m^2 , the complexity of the proton wave function, the tendency for cancellation in the expression (4.5) leading to νW_2 , and to a lesser extent the slow convergence of the integrals for νW_L (which, except for α_s variation would be logarithmically divergent) lead to the very large numerical multiplier of (5.15).

VI. $(1-x_{\text{Bj}})^4$ AND $(1-x_{\text{Bj}})^2/Q^2$ CORRECTIONS TO νW_2

To obtain the corrections V_2 and X_2 to the leading terms of νW_2 [see Eq. (4.27)] requires a major effort involving REDUCE.¹⁴ Our procedure is to isolate terms in A^+ which behave as

$$A^+ \underset{x \rightarrow 1}{\sim} a^+(1-x) + f^+(1-x)^2 + g^2 \frac{(1-x)}{Q} + \frac{h^+}{Q^2}. \quad (6.1)$$

Here a^+ is the leading term already discussed and we recall that the possible "leading" matrix-element terms b^+ through e^+ of (3.18) are found to be zero.

Contributions to V_2 arise through a^+f^+ interference in $|A^+|^2$ [recall phase space provides an additional $(1-x)$] as well as through trivial corrections to the $|a^+|^2$ leading term arises from the full x dependence in $d\Gamma^{(3)}$ of Eq. (4.11). The same diagram and γ -matrix configurations that contribute to a^+ (see Table IV) contain terms of the f^+ type as a result of keeping nonleading corrections in $(1-x)$ to the numerator and denominator algebra. However, there are also many new configurations of the A type that contribute to f^+ . (In axial gauge, B- and C-type diagrams do not contribute to f^+ .) Since we are concerned with an interference a^+f^+ contribution, only the same final helicity configurations $(+-+, ++-, +--, +++)$ that contribute to the leading term a^+ need be retained for f^+ . The structure of f^+ is revealed by the vector structures which appear

$$\begin{aligned} f_{+-+}^+ &\propto (\hat{L}^2 \hat{l}^2, \hat{L}\hat{l}, \hat{L}\hat{l}, 1), \\ f_{++-}^+ &\propto (\hat{L}^2 \hat{l}^2, \hat{L}\hat{l}, \hat{L}\hat{l}, 1), \\ f_{+--}^+ &\propto (\hat{L}^2 \hat{l}, \hat{L}\hat{l}^2, \hat{L}, \hat{l}), \\ f_{+++}^+ &\propto (\hat{L}^2 \hat{l}, \hat{L}\hat{l}^2, \hat{L}, \hat{l}). \end{aligned} \quad (6.2)$$

Each vector structure is multiplied by an associated invariant amplitude. In general, these invariant amplitudes are lengthy expressions. For the interference contribution V_2 we compute $a^+f^{++} + a^{++}f^+$ summed over final helicity states and integrated against the leading term in $d\Gamma^{(3)}$. We combine this with the trivial corrections to the a^{+2} term due to nonleading corrections to $d\Gamma^{(3)}$ to obtain the full result for V_2 . As for T_2 and V_2 , we find that the ratio V_2/S_2 is a slowly varying function of χ . We find, for the wave function (3.6),

$$\frac{V_2^n}{S_2^n} = \begin{cases} -96, & \chi=10, \\ -168, & \chi=400. \end{cases} \quad (6.3)$$

Unlike T_2/S_2 and U_2/S_2 the above ratio does, however, change in going to a neutron target. We find

$$\frac{V_2^n}{S_2^n} = \begin{cases} 15, & \chi=10, \\ 14, & \chi=400. \end{cases} \quad (6.4)$$

Note that the coefficients of the $(1-x_{\text{Bj}})^4$ correction are very large especially in the case of the proton and that, in fact, very large χ values (i.e., x_{Bj} very near 1) are required

for the combined S_2 and V_2 terms of the $(1-x_{\text{Bj}})$ power series to yield a positive result for νW_2^p .

Thus the behavior $\nu W_2^p \sim (1-x_{\text{Bj}})^3$ in the currently accessible $x_{\text{Bj}} < 0.9$ region could have little to do with off-shell counting arguments that apply to the leading $(1-x_{\text{Bj}})^3$ term discussed here. Positivity, of course, implies that the negative $(1-x_{\text{Bj}})^4$ term is partially canceled (at moderate x_{Bj}) by higher-power terms. This could leave an effective $(1-x_{\text{Bj}})^3$ power at moderate x_{Bj} values. Nonetheless our calculations show that the power-counting result for the leading S_2 term can only be strictly trusted at x_{Bj} values much nearer to 1 than those currently accessible to experiment.

On a related point, note that (6.3) and (6.4) imply that $\nu W_2^n / \nu W_2^p$ should approach the canonical value of $S_2^n / S_2^p = \frac{5}{7}$ (Ref. 12) from above. If anything, current data around x_{Bj} of 0.9 suggest that $\nu W_2^n / \nu W_2^p$ is below the value of $\frac{5}{7}$. Thus the asymptotic results for the $(1-x_{\text{Bj}})^4$ term obtained here would appear to obtain only at x_{Bj} , still nearer to 1.

In what follows we will adopt the optimistic point of view that the $(1-x_{\text{Bj}})^4$ term is largely compensated by terms with still higher powers. The $S_2(1-x_{\text{Bj}})^3$ term is the least-damped $(1-x_{\text{Bj}})$ behavior and a type of "duality" may hold in which this leading term also represents a good average of the sum of all terms. The higher-power corrections, T_2 and U_2 , discussed so far also have leading $(1-x_{\text{Bj}})$ behavior at their respective orders of $1/Q^2$. Our next computation will show a substantial correction to the $1/Q^2$ term at level $(1-x_{\text{Bj}})^2$, compared to the leading $(1-x_{\text{Bj}})/Q^2$ form. This correction could also be partially compensated by terms with still higher $(1-x_{\text{Bj}})$ powers. However, recall that the $(1-x_{\text{Bj}})/Q^2$ term vanishes for constant α_s , whereas the $(1-x_{\text{Bj}})^2/Q^2$ correction does not. In a sense the $(1-x_{\text{Bj}})^2/Q^2$ term is the first "non-trivial" higher-power correction at order $1/Q^2$.

We now turn to the $(1-x_{\text{Bj}})^2/Q^2$ correction term χ_2 of Eq. (4.27). Referring to (6.1) we find several possible sources for χ_2 :

- (a) a^+g^+ interference combined with a

$$\frac{1}{Q} \delta'(x-x_{\text{Bj}})(1-x)$$

phase-space correction [see (4.11)].

- (b) a^+h^+ interference combined with the leading

$$(1-x)\delta(x-x_{\text{Bj}})$$

phase-space term.

- (c) $|a^+|^2$ terms combined with phase-space terms of the form

$$\frac{(1-x)}{Q^2} \delta'(x-x_{\text{Bj}})$$

or

$$\frac{1}{Q^2} (1-x^2) \delta''(x-x_{\text{Bj}}).$$

- (d) a^+f^+ interference combined with

$$\frac{1}{Q^2} \delta'(x-x_{\text{Bj}})$$

or

$$\frac{1}{Q^2} (1-x) \delta''(x-x_{\text{Bj}})$$

phase-space terms.

All of these possible sources do, in fact, contribute. As for f^+ we confine ourselves to specifying the invariant-amplitude content of the new forms g^+ and h^+ , of (6.11), which contribute under (a) and (b). We find

$$\begin{aligned} g_{+-+}^+ &\propto \frac{\check{q}}{Q} (\hat{l}, \hat{L}, \hat{l}^2 \check{L}, \check{l} \hat{L}^2) + \frac{\hat{q}}{Q} (\check{l}, \check{L}, \check{l}^2 \hat{L}, \hat{l} \check{L}^2), \\ g_{+++}^+ &\propto \frac{\check{q}}{Q} (\hat{L}, \hat{l}, \hat{L}^2 \check{l}, \check{l}^2 \hat{L}) + \frac{\hat{q}}{Q} (\check{L}, \check{l}, \check{L}^2 \hat{l}, \hat{l}^2 \check{L}), \\ g_{+++}^+ &\propto \frac{\check{q}}{Q} (1, \check{L}, \check{l} \hat{L}) + \frac{\hat{q}}{Q} (\check{l} \check{L}, \check{L}^2, \check{l}^2), \\ g_{+--}^+ &\propto \frac{\hat{q}}{Q} (1, \check{L}, \check{l} \hat{L}) + \frac{\check{q}}{Q} (\hat{L} \hat{l}, \hat{L}^2, \hat{l}^2), \\ h_{+-+}^+ &\propto (\check{L} \hat{l}, 1), \\ h_{+-+}^+ &\propto (\hat{L} \check{l}, 1), \\ h_{+++}^+ &\propto (\check{L}, \check{l}), \\ h_{+--}^+ &\propto (\hat{L}, \hat{l}). \end{aligned} \quad (6.5)$$

The computation of the invariant amplitudes is performed using REDUCE.¹⁴ The expressions for those appearing in the g^+ amplitudes are lengthy while the ones contributing to the h^+ amplitudes are not as involved. The entire calculation of the interference and phase-space corrections listed under (a)–(d) is also performed by REDUCE with a final numerical integration yielding the results below. We employ the wave function (3.6) and obtain

$$\frac{X_2^p}{m^2 S_2^p} = \begin{cases} 696, & \chi = 10, \\ 898, & \chi = 400, \end{cases} \quad (6.6)$$

$$\frac{X_2^n}{m^2 S_2^n} = \begin{cases} 63, & \chi = 10, \\ 213, & \chi = 400. \end{cases}$$

We see that as in earlier cases the ratios are target sensitive but vary fairly slowly as a function of χ . The values given in (6.6) imply that the $(1-x_{\text{Bj}})^2/Q^2$ correction to the leading $(1-x_{\text{Bj}})^3$ behavior of νW_2 can be quite substantial. For $m^2 = 0.01 \text{ GeV}^2$ and $\Lambda_{\text{mom}} = 0.1 \text{ GeV}$, we have at $x_{\text{Bj}} = 0.9$,

$$\frac{\frac{1}{Q^2} X_2^p (1-x_{\text{Bj}})^2}{S_2^p (1-x_{\text{Bj}})^3} = \frac{6.96 \text{ GeV}^2}{Q^2 (1-x_{\text{Bj}})} = \frac{69.6 \text{ GeV}^2}{Q^2} \quad (6.7)$$

and

$$\frac{\frac{1}{Q^2} X_2^n (1-x_{\text{Bj}})^2}{S_2^n (1-x_{\text{Bj}})^3} = \frac{0.63}{Q^2 (1-x_{\text{Bj}})} = \frac{6.3}{Q^2}. \quad (6.8)$$

The proton X_2^p correction is clearly very sizable. Assuming that the 6.6-GeV² coefficient of (6.7) is not substantially varying as x_{Bj} decreases outside the range $x_{\text{Bj}} \geq 0.9$

(in which our calculation is perturbatively justified), we would obtain a $\sim 50\%$ correction at $Q^2=25 \text{ GeV}^2$, $x_{\text{Bj}}=0.5$.

We also remark that we have simply not attempted to extract the $1/Q^4$ correction to the leading $S_2(1-x_{\text{Bj}})^3$ term. Such a calculation is possible and we would again anticipate a large coefficient since there are many contributing sources from both nonleading phase-space corrections and direct-matrix-element terms.

VII. SUMMARY

In this paper we have explored in detail the predictions of perturbative QCD, using the approach of Refs. 4–6, for the behavior of the deep-inelastic structure functions for large x_{Bj} . We have compared the terms given below which derive entirely from the valence-quark wave-function states of the pion or nucleon target:

$$\nu W_2^\pi \underset{x_{\text{Bj}} \rightarrow 1}{\sim} S_2^\pi (1-x_{\text{Bj}})^2 + T_2^\pi / Q^2, \quad (7.1)$$

$$\nu W_L^\pi \sim S_L^\pi, \quad (7.2)$$

$$\begin{aligned} \nu W_2^N \sim & S_2^N (1-x_{\text{Bj}})^3 + T_2^N \frac{(1-x_{\text{Bj}})}{Q^2} + U_2^N \frac{1}{Q^4(1-x_{\text{Bj}})} \\ & + V_2^N (1-x_{\text{Bj}})^4 + X_2^N \frac{(1-x_{\text{Bj}})^2}{Q^2}, \end{aligned} \quad (7.3)$$

$$\nu W_L^N \sim S_L^N (1-x_{\text{Bj}})^3. \quad (7.4)$$

Since we are interested in the limit $Q^2 \rightarrow \infty$ followed by the limit of large x_{Bj} , we have systematically neglected terms of order $\alpha_s^2 (k_T^2 / (1-x_{\text{Bj}}))$ and $\alpha_s(Q^2)$ relative to terms of order $\alpha_s (k_T^2 / (1-x_{\text{Bj}}))$ in computing the various coefficient functions S_2, \dots, X_2 . In particular, the neglect of terms of order $\alpha_s(Q^2)$ implies that we need only consider diagrams, for the forward Compton amplitude, in which the photon enters and exits on the same quark line. Equivalently, in our calculations we sum incoherently the absolute squares of the tree-graph wave-function amplitudes (A^+ or A^-) for each type of quark in the bound state.

Aside from the initial-wave-function choice, for which we have taken the “weak-binding” forms (2.6) and (3.6) (there is no substantial sensitivity here, as discussed), there are two parameters in our calculation. The first is Λ_{mom} for which we have taken the value

$$\Lambda_{\text{mom}} = 0.1 \text{ GeV}, \quad (7.5)$$

in rough agreement with the lower range of existing determinations. (We use the lower range because our results indicate the likelihood of substantial higher-twist contamination in these determinations.) The second is the quark mass, which provides the infrared cutoff for internal-transverse-momentum wave-function integrals. The normalizations of S_2^N and S_2^π scale as $1/m^4$ and $1/m^2$, respectively, and thus provide a sensitive measure of m^2 . Comparing these quantities to approximate experimental determinations shows that

$$m^2 \lesssim 0.01 \text{ GeV}^2 \quad (7.6)$$

yields the correct normalization for both. The average transverse momentum of the quark struck by the deep-inelastic probe is exemplified by the results (4.26) which we approximate for discussion as

$$\langle k_T^2 \rangle^N \sim 3m^2, \quad (7.7)$$

roughly independent of x_{Bj} . The important point to note is that with (7.6) this is a small number entirely consistent with indirect determinations using fragmentation and similar data. Using (7.5) and (7.6) we find that all α_s arguments which appear in our calculations are well into the perturbative domain, provided $x_{\text{Bj}} > 0.9$.

Given such a small result for m^2 or $\langle k_T^2 \rangle$, it has become customary to think that the $1/Q^2$ power-law corrections (which scale as m^2 relative to leading terms) are then very likely to be small, especially corrections of this type which have no “extra” dynamical origin such as diquark¹⁵ or other nonperturbative internal wave-function structure. In this paper we have found that for a pion target this optimistic scenario appears to hold, whereas for a nucleon target one must anticipate large power-law corrections.

For the pion target we found ($x_{\text{Bj}} \geq 0.9$)

$$\frac{S_L^\pi}{m^2 S_2^\pi} \geq 0.2 \quad (7.8)$$

and for

$$r \equiv \frac{4x_{\text{Bj}}^2 W_L}{Q^2 W_2}, \quad (7.9)$$

related to σ_L by

$$\frac{\sigma_L}{\sigma_T} = \frac{r}{1-r}, \quad (7.10)$$

we obtain

$$r^\pi \underset{x_{\text{Bj}} \geq 0.9}{\geq} \frac{0.8m^2}{Q^2(1-x_{\text{Bj}})^2}. \quad (7.11)$$

For T_2^π we find a negligible result for $x_{\text{Bj}} \approx 0.9$ rising rapidly to the asymptotic value (independent of wave-function choice)

$$\lim_{x_{\text{Bj}} \rightarrow 1} \frac{T_2^\pi}{4S_L^\pi} = 1 \quad (7.12)$$

for which the $1/Q^2$ correction is purely longitudinal, as obtained in Ref. 4 in the absence of helicity-flip and mass corrections. At accessible x_{Bj} values our results imply that the $1/Q^2$ correction T_2^π to W_2^π is not pure longitudinal and is in any case negligible once the relationship between the normalizations of S_2^π and T_2^π through m^2 is taken into account. The estimate of W_L^π contained in the second work of Ref. 4, appropriate to moderate x_{Bj} , is a factor of 4 larger than our result at $x_{\text{Bj}}=0.9$ (see Fig. 4). Both evaluations are substantially lower than the original estimate in the first work of Ref. 4.

The most dramatic example of a large proton-target power-law correction is the result for r of (7.9). The leading term in the asymptotic series for r^p is found to be ($x_{\text{Bj}} \geq 0.9$)

$$r^p \sim \frac{4}{Q^2} \frac{S_L^p}{S_2^p} \gtrsim 1.6 \times 10^5 m^2 / Q^2 \quad (7.13)$$

[see (5.9)]. Since positivity requires $r \leq 1$, the higher terms in this asymptotic series must be important until $Q^2 > 1000 \text{ GeV}^2$. Certainly one can find no justification for the statement that small $\langle k_T^2 \rangle$ guarantees a small result for σ_L / σ_T . We have attempted in Sec. V to present enough calculational details that the sources of such a large result for S_L^N become apparent. These include: a large number of contributing diagrams; no cancellation tendency, whereas the S_2^N calculation exhibits some cancellation (which would, in fact, be complete for constant α_s and a weak-binding wave function); and slower integration convergence.

The interplay of these effects is quite subtle. For example, in going from the weak-binding wave function (3.6) to the form (3.8), the cancellation effect is reduced and S_2^p increases [see (4.21)]; nevertheless, at $\chi = 10$, r^p also increases. Thus it does not seem that the large value of r^p can be substantially reduced by minimizing the cancellation in S_2^p .

The terms T_2^N and U_2^N which have the most dominant $x_{Bj} \rightarrow 1$ behavior at the $1/Q^2$ and $1/Q^4$ level, respectively, in the series for W_2 , are found to be modest in size. As discussed they would be zero in the approximation of constant moving coupling constant. With the choice (2.21) we find (at $x_{Bj} \approx 0.9$)

$$\frac{T_2^N}{S_2^N} \approx -4m^2, \quad (7.14)$$

$$\frac{U_2^N}{S_2^N} \approx 70m^4$$

[see (4.22) and (4.23)]. At $Q^2 = 10 \text{ GeV}^2$ and $x_{Bj} = 0.9$ one obtains

$$\frac{T_2^N (1-x_{Bj})}{Q^2 S_2^N (1-x_{Bj})^3} \approx -0.4, \quad (7.15)$$

$$\frac{U_2^N (1-x_{Bj})^{-1}}{Q^4 S_2^N (1-x_{Bj})^3} \approx +0.7,$$

which can hardly be called small corrections. Nonetheless, they are smaller than the values preferred by Barnett in a fit of this type² which assumes a higher-twist correction form

$$\left[1 - \frac{7m^2 x_{Bj}}{Q^2 (1-x_{Bj})} + 600m^4 \frac{x_{Bj}^2}{Q^4 (1-x_{Bj})^2} \right]. \quad (7.16)$$

He obtains a good fit for $m = 0.138 \text{ GeV}$, while the x_{Bj} and x_{Bj}^2 factors reduce the "effective" $1/Q^2$ and $1/Q^4$ coefficients (in the x_{Bj} range of the fit) to values nearer those given in (7.14); it is clear that (7.16) suggests a larger positive $1/Q^2$ or $1/Q^4$ correction than predicted by T_2 and U_2 alone.

We have computed the coefficient of one possible term

which could provide a correction of the desired type. We find a $1/Q^2$ correction of the form

$$\frac{X_2^p (1-x_{Bj})^2}{S_2^p (1-x_{Bj})^3} \underset{x_{Bj} \approx 0.9}{\approx} \frac{700m^2}{Q^2 (1-x_{Bj})}. \quad (7.17)$$

(This ratio, unlike earlier ratios, is target sensitive—the neutron result is $\sim \frac{1}{10}$ as large.) Though less leading as $x_{Bj} \rightarrow 1$ than the $1/Q^2$ T_2 correction, the large coefficient implies that the X_2^p correction completely dominates the T_2^p correction for $x_{Bj} \leq 0.9$. We have not computed the $(1-x_{Bj})^2/Q^4$ term which is the natural competitor to the $U^2/Q^4(1-x_{Bj})$. There is a large number of sources for this form and it could easily dominate the latter.

Note that (7.17) is the only term we calculate that has a target-mass contribution. Defining

$$X_2^p = X_2^p \text{ twist } 4 + X_2^p \text{ target mass},$$

we find, using ξ scaling,

$$X_2^p \text{ target mass} = 3M_T^2 S_2^p.$$

Thus, in our weak-binding model with $m = 0.1 \text{ GeV}$, $M_T = 0.3 \text{ GeV}$ and the target-mass contribution to (7.17) is negligible. The correct procedure to determine the full value of X_2^p is to subtract the weak-binding value of $X_2^p \text{ target mass}$ and to add back in $X_2^p \text{ target mass}$ with the correct value of $M_T = 0.937 \text{ GeV}$. (This assumes that $X_2^p \text{ twist } 4 / S_2^p$, like V^p , is not strongly dependent on the wave function; we have not been able to verify this explicitly, since the complexity of computing X_2^p / S_2^p for other than weak binding is prohibitive.) This results in a 40% increase in X_2^p when $m^2 = 0.01 \text{ GeV}^2$. Thus, target-mass corrections alone underestimate the full X_2^p by a factor of more than 3.

Although the term (7.17) seems quite large we would like to point out that it is of precisely the form and general magnitude considered by Barnett² in his favored fits. Barnett adopted the higher-twist correction factor

$$(1 + x_{Bj}^3 W_0^2 / W^2), \quad (7.18)$$

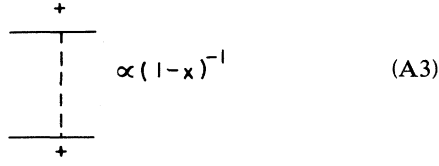
where

$$W^2 = Q^2 \frac{(1-x_{Bj})}{x_{Bj}}.$$

As $x_{Bj} \rightarrow 1$ this form is identical to our X_2 correction provided $W_0^2 = X_2 / S_2$. For an average nucleon target, $N \equiv (p+n)/2$ (as considered in Ref. 2), we use (6.6) and $S_2^N / S_2^p = \frac{3}{7}$ to yield our prediction,

$$(W_0^2)^N = X_2^N / S_2^N = 509m^2. \quad (7.19)$$

Barnett analyzed² three sets of data—European Muon Collaboration (EMC), CERN-Dortmund-Heidelberg-Saclay (CDHS), and SLAC-MIT—and obtained the following values of W_0^2 in (7.18) in combined "leading-order QCD" + "higher-twist" fits:

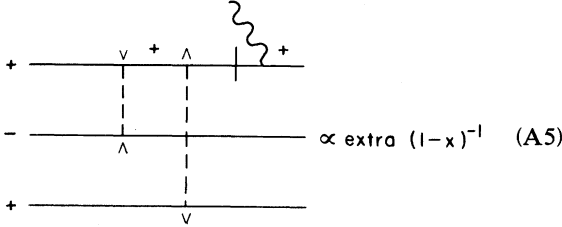


$$\propto (1-x)^{-1} \quad (\text{A3})$$

is proportional (in axial gauge) to the component of the momentum carried by the gluon and is thus proportional to $(1-x)^{-1}$. The final-state integral produces an extra suppression from the longitudinal-momentum-fraction integrals:

$$\int_0^\infty dx dz \cdots dz_{n-1} \delta(1-x-z-\cdots-z_{n-1}) \propto (1-x)^{n-2}. \quad (\text{A4})$$

Consider now the A^2 amplitude, which contributes to W_2 . For simplicity look at diagrams in which all the gluon lines are attached to the struck fermion line. We can always gain a factor of $(1-x)^{-1}$ (from the numerator algebra) for each gluon line which we can terminate with a $\hat{\gamma}$ on a negative-helicity-spectator line or with a γ on a positive-helicity-spectator line. We gain, in this way, a factor $(1-x)^{-(n-1)}$. Further enhancement is possible if we pair positive-helicity spectators and negative-helicity spectators as in

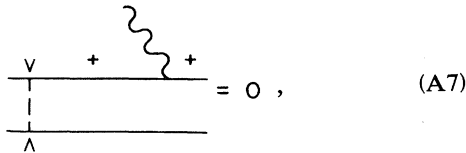


$$\propto \text{extra } (1-x)^{-1} \quad (\text{A5})$$

yielding an extra $(1-x)^{-1}$ [Eq. (A2)] for each such pair of opposite-helicity spectators. The number of such pairs is easily seen to be

$$\frac{1}{2}[(n-1)-2|\Delta\lambda|], \quad (\text{A6})$$

where $\Delta\lambda$ is the difference between the total helicity of the initial state and the helicity of the struck quark. Note that we cannot pair a spectator with the struck quark itself because



$$= 0, \quad (\text{A7})$$

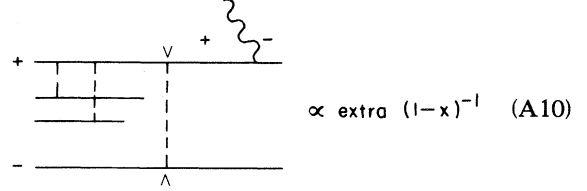
since $\gamma^{+2}=0$. Summing up all the $(1-x)$ powers yields

$$(1-x) \text{ power} = 2(n-1) - (n-1) - \frac{1}{2}[(n-1)-2|\Delta\lambda|] = \frac{1}{2}(n-1) + |\Delta\lambda| \quad (\text{A8})$$

for the A^+ amplitude. Computing $|a^+|^2 \times$ phase space (A4) yields

$$\begin{aligned} \nu W_2 &\propto_{x \rightarrow 1} (1-x)^{(n-1)+2|\Delta\lambda|+n-2} \\ &= (1-x)^{2n-3+2|\Delta\lambda|}. \end{aligned} \quad (\text{A9})$$

For νW_L the discussion is very similar, the only difference being that now we can get further numerator enhancement by pairing a spectator with the active quark provided they have opposite helicities in the following configuration:



$$\propto \text{extra } (1-x)^{-1} \quad (\text{A10})$$

Observe that the helicities have to be opposite because only in that case do we gain the power of \hat{q} that we need to obtain a leading contribution to W_L at the same time as we obtain $(1-x)^{-1}$ of (A1) from the spectator connection. We gain the extra $(1-x)^{-1}$ from the “+” “split” of (A10). Combining (A10) and (A5) we see that we gain one power of $(1-x)^{-1}$ from a “+” “split” for each pair of opposite-helicity fermions in the initial state, this time including the struck quark. This number is easily seen to be

$$\frac{1}{2}(n-2\Lambda_T), \quad (\text{A11})$$

where Λ_T is the total helicity of the initial state. Combining powers we get

$$\begin{aligned} \nu W_L &\propto |A^-|^2 \text{ phase space} \\ &\propto (1-x)^{2[2(n-1)-(n-1)-(n-2\Lambda_T)/2]+n-2} \\ &= (1-x)^{2n-4+2\Lambda_T}. \end{aligned} \quad (\text{A12})$$

APPENDIX B: RELATION TO OPERATOR-PRODUCT RESULTS

The technique most commonly employed to study higher-twist effects in deep-inelastic scattering is the operator-product expansion. There the tree-level hard processes which are relevant at twist 4 are¹⁷ the two quark diagrams of Fig. 6(a) and the four-quark diagrams of Fig. 6(b). In axial gauge the diagram of Fig. 6(ai) contributes to twist 2 and higher and the diagrams 6(aii) and 6(aiii) contribute to twist 4 and higher. All these diagrams are present in the tree graphs of our calculation. We have not included four-quark diagrams such as 6(b) because they are suppressed—by a power of $\alpha_s(Q^2)$. (They actually vanish in the weak-binding case since the gluon is always cut and radiation on-shell \rightarrow on-shell is impossible.) The

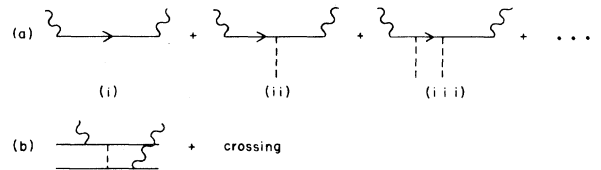


FIG. 6. Tree-level hard processes contributing to deep-inelastic scattering.

operator-product expansion automatically incorporates Lorentz invariance, gauge invariance, and the symmetry properties of the target.

In our direct calculation, symmetries and gauge invariance are not so explicit. It should be pointed out, however, that the weak binding calculation, when all spin-flip contributions are included, is completely Lorentz and gauge invariant. Gauge invariance follows immediately from the fact that, when the initial quarks are on shell, for fixed momenta of the final-state quarks, the total amplitude for absorption of a photon is gauge invariant. The use of the running coupling constant does not spoil this conclusion, because the coupling is the same for each gauge invariant subset of diagrams contributing to the amplitude. Once gauge invariance is established, Lorentz invariance follows immediately; because our calculation could have been done as well in Feynman gauge, where the axial vector η does not appear, and then, the only possible form of the answer is the one of Eq. (1.1). The use of axial gauge is a mere convenience and large portions of our calculations were also performed in Feynman gauge as an explicit check of our axial gauge results.

It is interesting to point out a difference between our result and that of Soldate.¹³ By calculating the matrix elements of the various operators, using large- x formalism, he finds as $x_{Bj} \rightarrow 1$

$$v W_2^{\text{HT}} \underset{x_{Bj} \rightarrow 1}{\propto} \frac{(1-x_{Bj})^2}{Q^2}$$

while we find

$$v W_2^{\text{HT}} \underset{x_{Bj} \rightarrow 1}{\propto} T_2 \frac{(1-x_{Bj})}{Q^2} + X_2 \frac{(1-x_{Bj})^2}{Q^2}.$$

The disagreement seems to derive from our use of the running coupling constant in the calculation; if we used a constant α_s , the coefficient T_2 vanishes.

As a final point note that we have obtained results for the absolute normalization of our higher-twist effects through the use of an explicit wave function calculated for large x_{Bj} using the formalism of Ref. 5. In this sense our results are less general than those of the operator-product formalism but do provide an explicit normalization of the contributions which appear therein.

¹R. M. Barnett, D. Schlatter and L. Trentadue, Phys. Rev. Lett. **46**, 1659 (1981); D. W. Duke and R. G. Roberts, Nucl. Phys. **B166**, 243 (1980); F. Eisele, M. Gluck, E. Hoffman, and E. Reya, Phys. Rev. D **26**, 41 (1982).

²R. M. Barnett, Phys. Rev. D **27**, 98 (1983).

³J. F. Gunion, P. Nason, and R. Blankenbecler, Phys. Lett. **117B**, 353 (1982).

⁴E. L. Berger and S. J. Brodsky, Phys. Rev. Lett. **42**, 940 (1979); E. L. Berger, S. J. Brodsky, and G. P. Lepage, in Proceedings of the Drell-Yan Workshop, Fermilab, 1983, p. 187 (unpublished).

⁵S. J. Brodsky and G. P. Lepage, Phys. Rev. D **22**, 2157 (1980).

⁶S. J. Brodsky, T. Huang, and G. P. Lepage, Report No. SLAC-PUB-2540 (unpublished); T. Huang, in *High Energy Physics—1980*, proceedings of the XXth International Conference, Madison, Wisconsin, edited by L. Durand and L. G. Pondrom (AIP, New York, 1981), p. 1000.

⁷S. Brodsky, M. Scadron, J. F. Gunion, and N. Fuchs (unpublished). See S. Brodsky, in *Quantum Chromodynamics*, proceedings of the Summer Institute on Particle Physics, SLAC, 1979, edited by A. Mosher (Report No. SLAC-224, 1980), Appendix.

⁸W. Celmaster and D. Sivers, Phys. Rev. D **23**, 227 (1981).

⁹See, for example, the NA3 determination of $f_\pi(x)$. D. DeCamp, in *High Energy Physics—1980*, proceedings of the XXth International Conference, Madison, Wisconsin (Ref. 6),

p. 147.

¹⁰See Refs. 1 and 2, and G. Wolf, in *Proceedings of the 21st International Conference on High Energy Physics, Paris, 1982*, edited by P. Petiau and M. Porneuf, J. Phys. (Paris) Colloq. **43**, C3-525 (1982); F. Eisele, *ibid.* **43**, C3-337 (1982).

¹¹S. J. Brodsky, T. Huang, and G. P. Lepage, in *Quarks and Nuclear Forces* (Springer Tracts in Modern Physics, Vol. 100), edited by G. Höhler (Springer, Berlin, 1982), p. 81.

¹²G. R. Farrar, and D. R. Jackson, Phys. Rev. Lett. **35**, 1416 (1975).

¹³M. Soldate, Nucl. Phys. **B223**, 61 (1983).

¹⁴A. C. Hearn, Stanford University Report No. ITP-247, 1968 (unpublished).

¹⁵L. F. Abbott, W. B. Atwood, and R. M. Barnett, Phys. Rev. D **22**, 582 (1980); I. A. Schmidt and R. Blankenbecler, *ibid.* **16**, 1318 (1977); L. F. Abbott, E. L. Berger, R. Blankenbecler, and G. L. Kane, Phys. Lett. **88B**, 157 (1979).

¹⁶R. M. Barnett (private communication).

¹⁷R. L. Jaffe and M. Soldate, Phys. Lett. **105B**, 467 (1981); S. P. Luttrell, S. Wada, and B. R. Webber, Nucl. Phys. **B188**, 219 (1981); E. V. Shuryak and A. I. Vainshtein, *ibid.* **B199**, 451 (1982); R. L. Jaffe, Phys. Lett. **116B**, 437 (1982); Nucl. Phys. **B229**, 205 (1983); R. L. Jaffe and M. Soldate, Phys. Rev. D **26**, 49 (1982); R. K. Ellis, W. Furmanski, and R. Petronzio, Nucl. Phys. **B207**, 1 (1982). This contains a treatment of twist 4 based on transverse-momentum effects as well.